ISSN 2005-9043

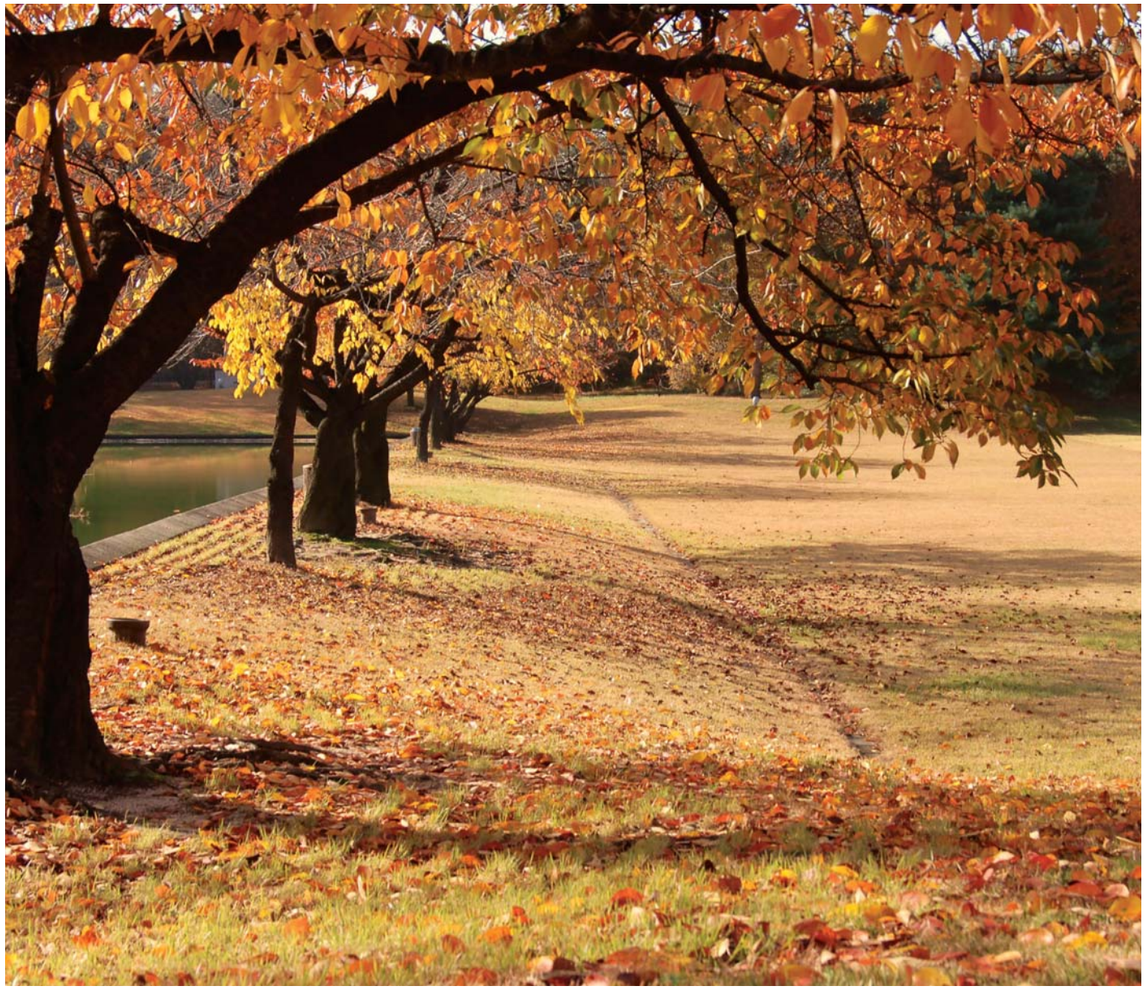

Cover story. Autumn at KIST

Vol. 4 No. 2 October 2011

KISTtoday

Leading to the world of tomorrow

contents

Foreword

The changes experienced by KIST over the last 45 years have been breathtaking. Initially in the 1960's, KIST sent its scientists to America to hone their research skills and techniques in order to bring a higher level of expertise back to Korea. During this period, Batelle Memorial Institute not only supported KIST's development, it also provided a model for investigating emerging areas of science and commercializing the technologies associated with related research. The knowledge gained through this association with Batelle was invaluable to KIST as it looked at pratical solutions for spurring the nation's economic development.

The rest is history. Korea's economy has exhibited extraordinary growth over a short period of time, thanks in large part to the innovative technologies developed at KIST and transferred to Korean industries. Now scientists and government officials from developing countries around the world are coming to KIST for inspiration and opportunities to learn, just as we once sought advice and support from research giants like Batelle.

This issue of *KISToday* looks at our history and what we can learn from it. We want to retrace what has occurred in our major areas of research, some of our most significant achievements, and how we are using our strengths in emerging areas of research which will define KIST's future path and ensure sustained economic growth for our country. Scientists who respond to the pressing challenges of the times and bring honor to their country in the process are just as prevalent at KIST now as they were in our early years. Their passion and exceptional ideas are clearly on display in the articles describing their work in this issue.

President **Kil-Choo Moon**

Visualizing Biological Molecules: Seeing is Believing!

Hyesung Jeon

[a]Optoelectronic Materials Center

•

idkim@kist.re.kr

We have all seen pictures of cells in textbooks, journal articles, newspapers, and even in TV shows about criminal investigations. This detailed visualization has been made possible over the last 50 years or so through electron microscopy, which shows specific features within individual cells.

Electron microscopy (EM) is one of the techniques used to see small molecules at better resolution, covering a wide range between 10^{-3} ~ 10^{-9}m (Figure 1). There are some differences in the methods used for EM in material or biological science, but generally speaking, it is the preferred tool to use for observing something large (in the size of mm or μm) at high resolution (nm level). In the structural biology field, X-ray crystallography has been the traditional technique to show the atomic resolution structure of biomolecules, and NMR (nuclear magnetic resonance) spectroscopy has the advantage of being able to see the dynamics of molecules, but EM is considered to be the most comprehensive technique for seeing the "ultra-structure" of macromolecules in biological systems.

The first step of microscopy is to see an object, with the ultimate aim of seeing it better and in its most natural state. Thus a specimen should be well preserved, which is why the cryo method was developed for most biological samples. In order to freeze samples in their natural states, freezing techniques and equipment were developed for specimen preparation (e.g. high pressure freezer). When samples of any kind are preserved in a fully hydrated state, we are better able to observe their

(a) Sewing needle
(b) Human hair
(c) Thin section of mammalian cell
(d) Bacterial cells
(e) Herpes viruses
(f) Enzyme macromolecule by processing
(g) Defect in graphite

FIGURE 1. Range of resolution of various magnifying tools and cryo-TEM at KIST

internal three-dimensional structures, which will then enable us to understand their biological functions.

EM uses transmission or scanning electron microscopes (TEM or SEM) for seeing the images of thin sections of the specimen or its scanned surface by means of transmitted electron beams. Cryo-EM refers to specimen preparation and observation at cryo-temperatures, usually -170℃. The biomolecules can be preserved by vitreous (amorphous) ice in this cryo system, so this method is particularly effective at

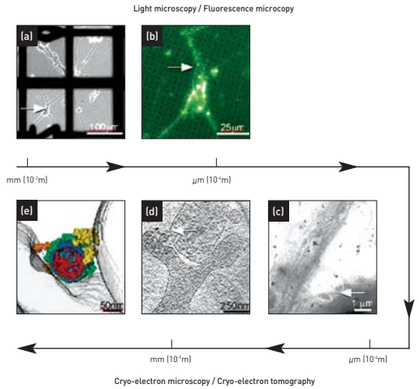

FIGURE 2. Combination of wide-range light microscopy and high-resolution electron microscopy

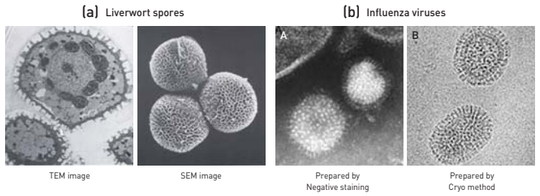

FIGURE 3. Different imaging and preparation techniques

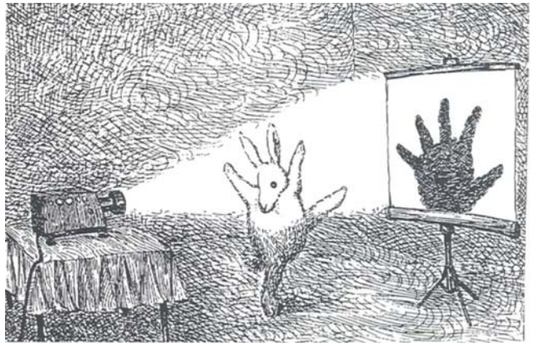

FIGURE 4. (from "Crystallography Made Crystal Clear" by G. Rhodes, in page 19, 'Fun in reciprocal space. Drawing by John. O'Brien; 1991, The New Yorker Magazine)

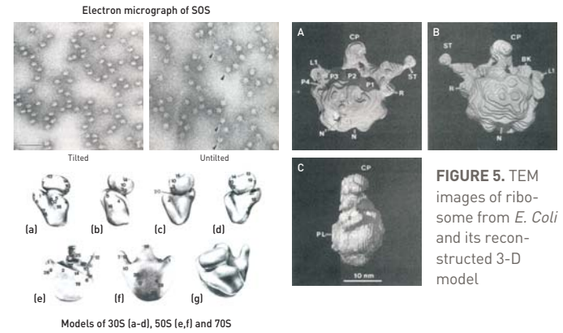

FIGURE 5. TEM images of ribosome from *E. Coli* and its reconstructed 3-D model

showing the structure in its natural state without removing or replacing the water portion of the specimen.

EM images are a 2-D projection of 3-D objects. Compared to other structural biology techniques, x-ray diffraction or NMR spectroscopy, EM has the advantage of direct observation without calculation of diffraction pattern or spectrum. However, seeing 2-D images is inadequate for seeing the entire structure of 3-D molecules. As seen in Figure 4, there is ambiguity in 2-D projections. Figure 4 illustrates the difference in reciprocal space, leaving us to wonder at the three-dimensional structure represented by the projection.

Thanks to technical developments, we can now "reconstruct" the 3-D structure of biological molecules from the 2-D images taken by EM. Currently, the 3-D EM reconstruction field has two main branches, one focused on single-particle reconstruction, the other on electron tomography. Single-particle reconstruction analyzes the 3-D structure of a target molecule and was the principal method used in the past before the tomography technique was developed. Ribosome, the protein-making macro-machine, has often been used as the subject in EM studies (Figure 5).

A specimen used in single particle reconstruction is usually purified to eliminate all but one species. Different projections are shown depending on the positions of particles on the EM sample grids. Each particle in the raw images is selected, aligned and grouped into classes according to similar characteristics. The class-averaged images are then used to build up a 3-D model by including orientations. By rotating the specimen holder inside the electron microscope, tilted images at consecutive angles from the projection screen are put through the same process.

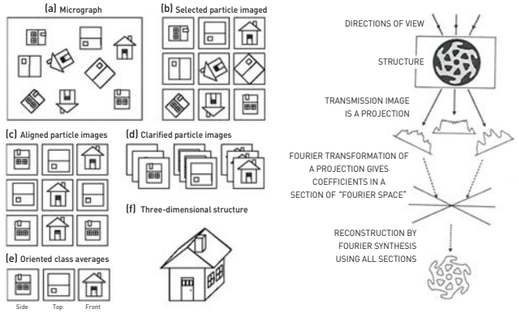

FIGURE 6. Schemes illustrating the theory behind 3-D reconstruction

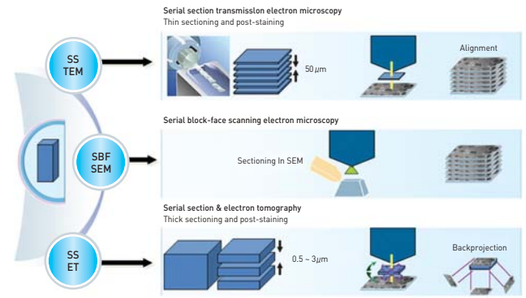

FIGURE 7. Preparation methods for tomography

The purpose of tomography is to reconstruct the whole interior of a biological specimen. Since TEM uses a transmitted electron beam, the resulting projections reflect information about the inside particles. By TEM images from tilting series over ±70℃, we can reconstruct a specimen as thick as ~500 nm. To prepare a specimen for 3-D tomography, several methods can be used to see the targeted width and thickness in the samples. The conventional method is to make serial sections and take TEM images, then align and stack them all up to the original thickness of the specimen. We can also use SEM images; however, this choice depends on how thin the sections are that can be imaged in SEM since we can see only surface images with SEM. Another method is to use a high-voltage electron microscope, which has higher penetration power, and thus is able to get more information from a thick specimen which can then be used to identify its thicker 3-D structure.

There have been continuous efforts to observe larger-size biomolecules at higher resolution to see how those molecules perform their functions inside the body. Each method used in exploring structural biology has unique advantages and disadvantages. Since a kind of plateau has been reached in further developing these methodologies, now we are trying to combine existing methods (so called "hybrid" methods) to obtain only the advantages from each. In the future, these hybrid methods, including techniques to examine larger molecules at better resolution, will be the key imaging techniques.

X-ray crystallography and cryo-electron microscopy have made good partners due to combining the advantages of the atomic resolution used in crystallography with the greater perspective gained from microscopy. In this way, the whole structure of macromolecules and the specific amino acid residues in their active sites can be seen. Similarly, NMR showing the high resolution structure plus dynamic aspects of molecules can be another partner with cryo-EM. By using electron tomography to define the organelle structure, the positions, population and moving paths of target proteins can be mapped with different imaging techniques.

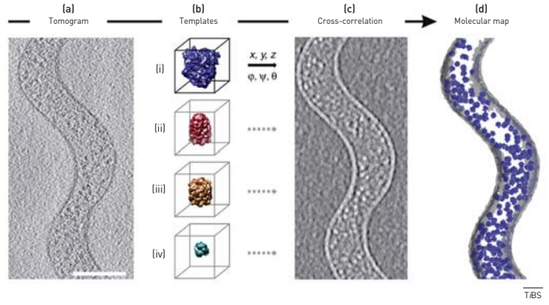

FIGURE 8. Example of mapping proteins by combining crystallography and electron microscopy

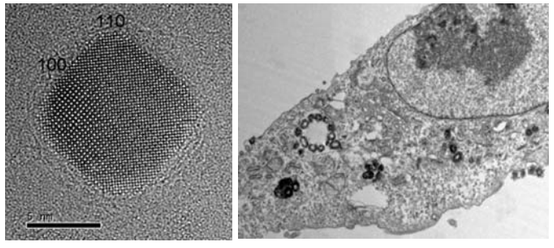

FIGURE 9. Characterization of a material by itself and in the cell

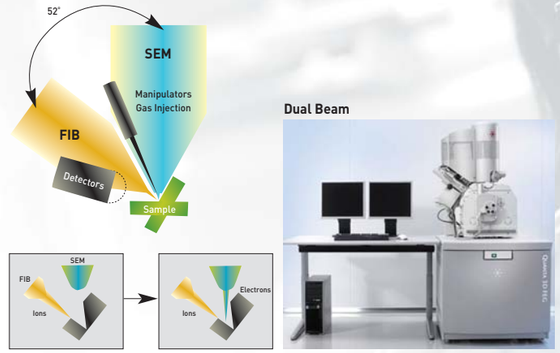

FIGURE 10. Dual-beam cryo/FIB: schematic representation and photo of the equipment used at KIST

New frontiers of science are opening by fusing nano- and bio-technology. Material science researchers have used TEM and SEM for a long time and have developed methods of analysis tailored specifically to their field. The resolution achieved in material EM is much higher than in biological microscopy, since biomoleules are considerably softer than material molecules and do not have electron-dense particles. Nano-technology allows us to look at how nano materials exist and behave in cells or organelles, which is encouraging the development of methods combining material and biological microscopy in order to see both kinds of molecules at the same time. Currently, many images accompanying published journal articles reflect the use of these electron microscopic methods.

Embracing the new trends in microscopic studies, KIST is well positioned to lead in this field. The cryo-TEM at KIST is the best cryo electron microscope in the country and is equipped with tomography functions. The cryo-FIB (Focused Ion Beam)/SEM, recently set up at KIST, is also rarely seen around the world. With this type of innovative equipment at hand, a strong focus of research at KIST is to combine material and biological specimens, perform nano-analysis and develop a better understanding of structural biology. Few research institutes in the world have resources equaling KIST's to support this type of important molecular study.

This detailed visualization has been made possible over the last 50 years or so through electron microscopy, which shows specific features within individual cells.

REFERENCES

1. Leis A, Rockel B, Andrees L, Baumeister W., Trends Biochem Sci. 2009 Feb;34(2):60-70.
2. Steven AC, Baumeister W., J Struct Biol. 2008 Sep;163(3):186-95.
3. Rhodes G (1993) *Crystallography Made Crystal Clear*. San Diego, CA: Academic Press.
4. Bozzola JJ, Russell LD (1999) Electron Microscopy. Sudbury, MA: Jones and Bartlett Publishers
5. Aloy P, Russell RB, Nat Rev Mol Cell Biol. 2006 Mar;7(3):188-97.

Tailoring Links between TiO_2 Hollow Hemispheres for Highly Sensitive Gas Sensors

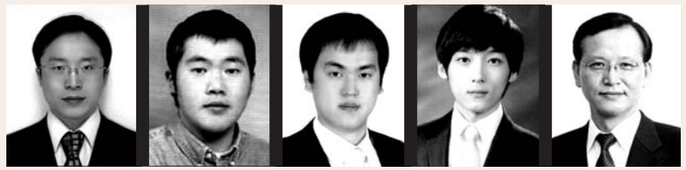

Ho Won Jang, Hi Gyu Moon, Young-Seok Shim, Do Hong Kim, Seok-Jin Yoon

Electronic Materials Research Center

•

hwjang@kist.re.kr

Introduction

Semiconducting metal oxide gas sensors are of great interest due to their simple fabrication processes, low cost, small size, and high sensitivity [1]. Titanium oxide (TiO_2) is a promising material for use in sensors that detect a variety of reducing gases, such as CO, H_2, H_2S, alcohols, and hydrocarbons, as well as oxidizing gases, including NO_x, O_3, and O_2 [2]. To achieve high-sensitivity sensors, the sensing material should exhibit a large surface-to-volume ratio and be highly accessible to gas molecules at the material's surface [3]. Accordingly, a wide variety of porous TiO_2 materials based on nanoparticles [4], nanowires [5], nanotubes [6], nanobelts [7], or nanofibers [8] has been intensively investigated for gas sensor applications. Because porous materials are usually synthesized using wet chemical methods, achieving large-area uniformity and compatibility with well-established semiconductor production processes has remained challenging.

An alternative method for achieving highly sensitive metal oxide gas sensors is soft-templating [9], which utilizes nanostructured inorganic or organic materials as sacrificial templates for the preparation of porous metal oxides. Fabrication of macroporous TiO_2 films [10] and hollow TiO_2 tubes [11] using soft templates and their use in gas-sensing materials have been reported recently. In these porous materials, which are composed of assemblies of individual micro/nanostructures, the structure of the links or necks between individual micro/nanostructures is a critical factor for determining the gas-sensing properties of the material. However, no systematic studies have yet clarified the role of links between individual micro/nanostructures in the gas-sensing properties of a porous metal oxide matrix. Here we present a strategy for enhancing the gas-sensing performance of a microporous TiO_2 material made by colloidal templating.

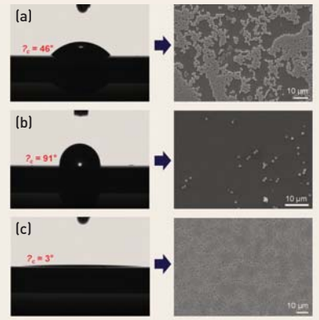

FIGURE 1. Photographs of water drops and SEM images of spin-coated polystyrene microspheres on (a) an as-cleaned SiO_2/Si substrate, (b) a HMDS-coated SiO_2/Si substrate, and (c) an O_2-plasma-treated SiO_2/Si substrate. Contact angles are displayed in each image

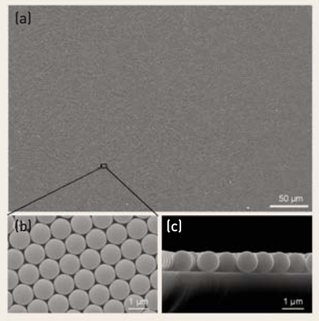

FIGURE 2. (a) Plain-view SEM image of a large-area colloid template of monolayer polystyrene microspheres on a SiO_2/Si substrate. Enlarged (b) plain-view and (c) cross-sectional SEM images.

Large-area polystyrene microsphere templates

Offering an effective method of large-area colloidal templating is a critical step for real device applications of colloid-templated metal oxide thin films. The surface wettability of three types of substrates was evaluated by measuring the contact angles of the water/solid interfaces. Figure 1 shows side-view photographs of water drops on the three substrates. The contact angle (θ_c) of the as-cleaned SiO_2/Si substrate is 46°, which is intermediate between hydrophilic ($0° \leq \theta_c \leq 30°$) and hydrophobic ($\theta_c \geq 90°$) surfaces. The HMDS-coated substrate shows a hydrophobic surface with θ_c= 91°, while the surface of the O_2-plasma-treated substrate is fully hydrophilic (θ_c= 3°). Such different surface conditions lead to completely different colloid templates, as shown in Fig. 1a-c. On the as-cleaned substrate, there are many irregular sphere-free regions. Only about half of the area is covered by the microspheres. On the HMDS-coated substrates, a few microspheres remain after spin coating. In contrast, closely packed microspheres are observed on the O_2-plasma-treated substrate.

Figure 2 shows a scanning electron microscopy (SEM) micrograph of the microspheres on the SiO_2/Si substrate that was fabricated using the O_2 plasma treatment. Over 250 um x 400 um area, there is no sphere-free regions. To the best of our knowledge, no previous work has shown such a large-area colloid template of monolayer microspheres. This result strongly suggests that achieving a hydrophilic surface prior to colloid deposition is pivotal for the formation of monolayer colloid templates. Since the suspension of the polystyrene spheres is aqueous, the suspension could be spread very well on the hydrophilic surface. In addition, the O_2-plasma-treated surface must be negatively charged with oxygen ions. Thus, relatively positive-charged microspheres in the suspension adhere to the substrate by the Coulombic interaction. It is proposed that the O_2 plasma pretreatment is a very useful method for obtaining large-area colloidal templates.

TiO_2 hollow hemispheres with tailed links

A schematic diagram showing the structure of the links between polystyrene microspheres as a function of O_2 plasma etching is shown in Figure 3a. Onto a close-packed monolayer of polystyrene microspheres (Figure 3b), O_2 plasma was then used to etch the surface regions of the beads by forming H_2O, CO, and CO_2 gaseous byproducts. The etching rate was not isotropic over the microspheres. The top surface experienced the highest etch rate and the bottom surface was not etched. The etch rate near the links was less than the etch rates on the perimeter side regions. As a result, the links between the microspheres became elongated narrow nanolinks during O_2 plasma etching for 2 min (Figure 3c). The links completely disappeared after etching for 4 min (Figure 3d). The surfaces of the microspheres became rougher dur-

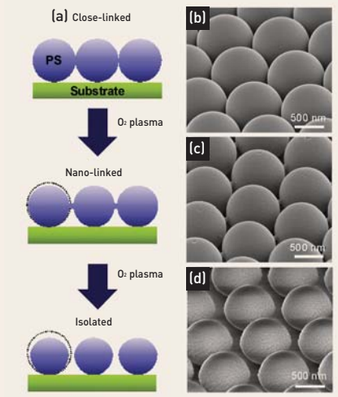

FIGURE 3. (a) A schematic drawing illustrating the link structures between polystyrene microspheres as a function of O_2 plasma etching time. (b-d) 52°-tilted-view SEM images of microsphere templates (b) before O_2 plasma etching and after (c,d) 02 plasma etching for (c) 2 min and (d) 4 min.

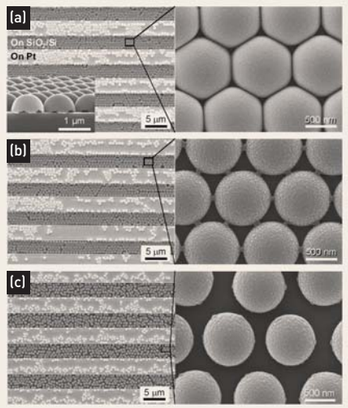

FIGURE 4. Plain-view SEM images of microporous TiO_2 films on Pt IDE-patterned SiO_2/Si substrates (a) without O_2 plasma etching, or with O_2 plasma etching for (b) 2 min and (c) 4 min.

ing the O_2 plasma etching, probably due to the heat generated by the exothermic reactions that formed H2O, CO, and CO_2.

A TiO_2 film was deposited on the plasma-treated polystyrene microsphere templates by rf sputtering at room temperature, and the samples were then calcined at 550℃ for 1 h to produce porous TiO_2 films with closed-linked hollow hemispheres (CHH), nanolinked hollow hemispheres (NHH), or isolated hollow hemispheres (IHH). Figure 4 shows plain-view SEM images of porous TiO_2 films on the Pt-IDE-patterned SiO_2/Si substrates. The porous film without O_2 plasma etching of the microsphere template reveals close-packed hemispheres on the patterned SiO_2/Si surface, whereas relatively sparse packing of hemispheres is observed on the Pt surface (Figure 4a). It is noted that the gas sensitivity is not affected by the film deposited on the Pt IDE, but is determined by the film deposited on the SiO_2/Si surface. The widths of links between CHH were 300-400 nm, and the lengths were less than 10 nm. O_2 plasma etching of the microsphere template for 1 min decreased the widths of links between CHH to 100-200 nm and increased the lengths to 30-50 nm. The widths and lengths of links between NHH on the microporous film submitted to O_2 plasma etching for 2 min (Figure 4b) were determined to be 30-80 nm and 40-70 nm, respectively. O_2 plasma etching for 3 min resulted in disappearance of the links between NHH, which produced IHH (Figure 4c). The spacings between IHH varied widely from 200 nm to 400 nm.

The microstructure of the microporous TiO_2 films was characterized by transmission electron microscopy (TEM). Figure 5a shows a cross-sectional TEM image of an embossed TiO_2 IHH film, which reveals that the hemispheres are hollow and crescent-shaped. The enlarged view displays that the bottoms of the hemispheres fold into the hollow inner space. Because the bottoms were too thin to support the hollow structures, they bent inward during the calcination. Clearly, a film was deposited directly on the substrate between the IHH. The TEM image in Figure 5b shows that the film is polycrystalline with a grain size of 10-30 nm. The selected area electron diffraction (SAED) pattern shown in Figure 5c indicates the polycrystalline nature of the TiO_2 films. The SAED pattern could be indexed as a pure anatase phase of TiO_2 ($I4_1/amd$ (No.141), JCPDS 84-1286) with lattice constants a = 3.7822 Å and c = 9.5023 Å. The high-resolution TEM image in Figure 5d clarifies that the film is tetragonally structured TiO_2 with an interplanar spacing of 0.351 nm for the (011) planes.

Gas sensing properties of TiO_2 hollow-hemisphere films

The responses (defined here as R_{air}/R_{gas}, where R_{gas} and Rair denote the sensors' resistance in the presence and absence of a test gas, respectively) of the microporous TiO_2 hollow-hemisphere films toward 500 ppm CO and ethanol gases are plotted in Figure 6. Compared to a reference flat TiO_2 film, all microporous TiO_2 hollow-hemisphere films show higher responses to CO and ethanol. However, the responses vary significantly with the type of links between TiO_2 hollow hemispheres.

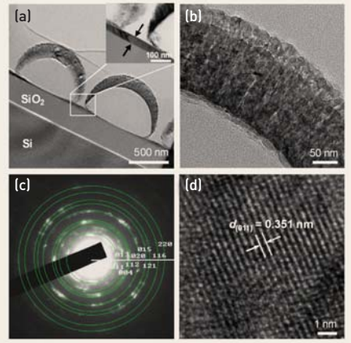

FIGURE 5. (a) Cross-sectional TEM image of isolated TiO_2 hollow hemispheres. (b) High magnification TEM image. (c) Selected area electron diffraction pattern. (d) High resolution TEM image.

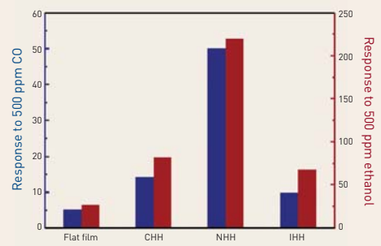

FIGURE 6. Responses of flat and microporous TiO_2 films to 500 ppm CO or ethanol.

Considering that all the microporous films had similar specific surface areas, the strong variation in response is very interesting. This result suggests that an additional key factor determines the response of microporous films, aside from the large specific surface area. By tailoring the links between hollow hemispheres, the maximum response ratio is as large as 7. Although several reports [12,13] have pointed to the importance of links or necks between individual micro/nanostructures in enhancing the gas-sensing performance of porous metal oxide materials, such an enhancement in gas sensitivity by tailoring the links has not been reported previously. The highest responses to CO and ethanol gases were obtained from the microporous film with NHH prepared through O_2 plasma etching of the microsphere template for 2 min. The responses of the film are 1.33, 3.39, 11.0, and 50.9 to 1, 5, 50, and 500 ppm CO, respectively, and 4.0, 17.5, 71, and 219 to 1, 5, 50, and 500 ppm ethanol, respectively. These responses are higher than those of high-sensitivity sensors based on TiO_2 nanoparticles (17 to 500 ppm CO and 65 to 47 ppm ethanol at 450℃) [14], TiO_2 nanotubes (8.5 to 500 ppm CO and 24 to 47 ppm ethanol at 450℃) [14], and TiO_2 nanofibers (4.4 to 25 ppm CO at 200℃) [15].

The strong dependence of the responses of the microporous TiO_2 films on the links between hollow hemispheres can be explained as follows. The morphology of the microporous films transformed from CHH, to NHH, to IHH as the O_2 plasma etching time increased. Current in the CHH films flows along the hemispheres. The links between CHH hinder the current flow because the adsorption of oxygen molecules induced surface band bending, which raises potential barriers to current flow, as illustrated in Figure 7a. The heights of the potential barriers are reduced by exposure to CO, leading to a decrease in the resistance. The modulation of the potential barriers, therefore, determines the response of the CHH films. Links in the NHH films are narrow and elongated. Then potential barriers at the nanolinks can be modified as shown in Figure 7b. With the longer width of the fully electron-depleted region, the current flow through the flat-top potential barriers became lower than that through the potential barriers in the CHH films, leading to the higher resistance in air. Upon exposure of the NHH film to CO, the potential barriers decrease as they do in the CHH film. However, the change of the resistance is more pronounced in the NHH film, as estimated using the area between the conduction band edges before and after exposure to CO. Thus, the higher response of the NHH film compared to the CHH film is attributed to the more efficient modulation of the potential barriers at the nanolinks. In the IHH film, current barely flows along the hemispheres because the current path is longer and has a higher resistance than the path through the IHH links. Consequently, remarkable potential barriers like those between CHH or NHH are no longer present, as shown in Figure 7c, resulting in lower responses. The response of the IHH film was still higher than the response of the plain reference film because the width of current paths in the IHH film (50-400 nm for the film with O_2 plasma etching for 3 min) is much narrower than that in the plain reference film (1.5 mm) and

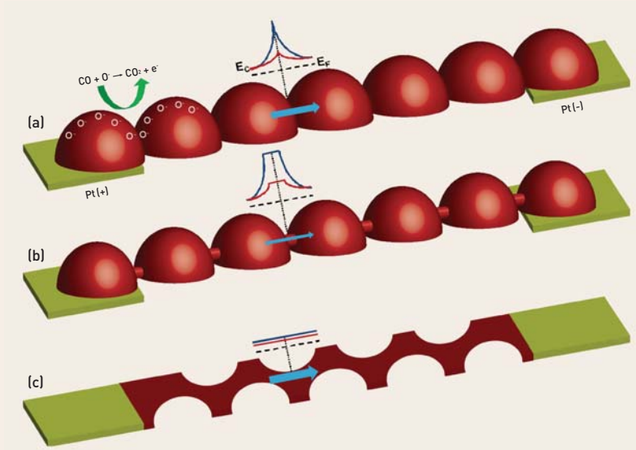

FIGURE 7. Schematic drawings of the major current path between Pt electrodes for microporous TiO_2 films with (a) CHH, (b) NHH, and (c) IHH.

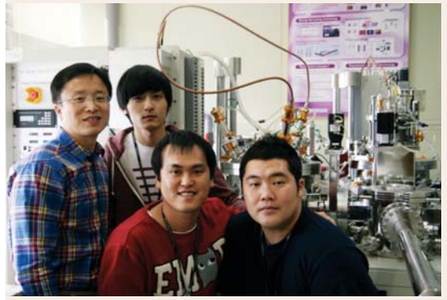

approaches the Debye length of TiO_2 (~25 nm).

The feasibility of using the micoporous TiO_2 films as reliable gas sensors was evaluated by measuring the sensing performance of the embossed TiO_2 NHH film at the operation temperature (250℃) for 10 days. Deviations in both the baseline resistance in dry air and the response to 50 ppm CO were less than 5%, which was comparable to the magnitude of the ripple signal in our measurement system. Such good thermal stability resulted from the chemical stability of the anatase TiO_2 at elevated temperatures as well as the calcination process at 550℃, which was much higher than the operation temperature of 250℃. In addition, because the NHH are separated from one another, the film is free from agglomeration among NHH, even after long-term operation.

Conclusion

We have demonstrated a method for synthesizing highly-ordered films composed of anatase TiO_2 hollow hemispheres by the soft templating technique using polystyrene microspheres. The structure of the links between hollow hemispheres could be controlled by O_2 plasma etching on the microsphere templates. This approach revealed a strong correlation between a film's gas sensitivity and the link structure. Our experimental results emphasize that the surface-to-volume ratio of an ensemble material composed of individual micro/nanostructures is not the only important factor. The links between individual micro/nanostructures play a critical role in modulating the sensing properties of the material. In addition to this general finding, the proposed synthesis method's facileness, large-scale productivity, and compatibility with semiconductor production processes hold promise for future applications of the embossed TiO_2 films in high-quality sensors, batteries, solar cells, and photocatalytic water splitting systems.

We have demonstrated a method for synthesizing highly-ordered films composed of anatase TiO_2 hollow hemispheres by the soft templating technique using polystyrene microspheres. The structure of the links between hollow hemispheres can be controlled by O_2 plasma etching on the microsphere templates.

NOTE

This article is based on our recent papers: Sens. Actuators B 149, 116 (2010) and J. Phy. Chem. C 115, 9993 (2011).

REFERENCES

1. G. Eranna, B. C. Joshi, D. P. Runthala, R. P. Gupta, Crit. Rev. Solid State Mater. Sci. 29, 111. (2004).
2. N. Yamazoe, K. Shimanoe, Sens. Actuators B 138, 100 (2009).
3. G. Korotcenkov, Sens. Actuators B 107, 209 (2005).
4. Y. F. Zhu, J. J. Shi, Z. Y. Zhang, C. Zhang, X. R. Zhang, Anal. Chem. 74, 120 (2002).
5. C. S. Rout, G. U. Kulkarni, C. N. R. Rao, J. Phys. D 40, 2777 (2007).
6. O. K. Varghese, D. W. Gong, M. Paulose, K. G. Ong, C. A. Grimes, Sens. Actuators B 93, 338 (2003).
7. Y. Wang, G. Du, H. Liu, D. Liu, S. Qin, N. Wang, C. G. Hu, X. Tao, J. Jiao, J. Wang, Z. L. Wang, Adv. Funct. Mater. 18, 1131 (2008).
8. I. D. Kim, A. Rothschild. B. H. Lee, D. Y. Kim, S. M. Jo, H. L. Tuller, Nano Lett. 6, 2009. (2006).
9. X. W. Lou, L. A. Archer, Z. C. Yang, Adv. Mater. 20, 3987 (2008).
10. Y. Wan, D. Y. Zhao, Chem. Rev. 107, 2821, (2007).
11. G. M. Kim, S. M. Lee, G. H. Michler, H. Roggendorf, U. Gsele, M. Knez, Chem. Mater. 20, 3085 (2008).
12. G. Korotcenkov, Mater. Sci. Eng. B 139, 1 (2007).
13. V. V. Sysoev, T. Schneider, J. Goschnick, I. Kiselev, W. Habicht, H. Hahn, E. Strelcov, A. Kolmakov, Sens. Actuators B 139, 699 (2009).
14. M. H. Seo, M. Yuasa, T. Kida, J. S. Huh, K. Shimanoe, N. Yamazoe, Sens. Actuators B 137, 513 (2009).
15. J. A. Park, J. Moon, S. J. Lee, S. H. Kim, T. Zyung, H. Y. Chu, Mater. Lett. 64, 255 (2010).

Traffic-Related Air Pollution Research at KIST

Seung-Bok Lee, Hyoun-Cher Jin, Gwi-Nam Bae
Environmental Sensor System Research Center
•
gnbae@kist.re.kr

Introduction

Vehicle exhaust is considered a major air pollution source in urban areas, particularly in mega-cities like Seoul. The number of registered vehicles nationwide in Korea at the end of 2010 was about 18 million, that is, one vehicle per 2.8 persons. Public health is being threatened by high concentrations of hazardous substances in vehicle exhaust [1], which are not sufficiently diluted before exposure to humans. The Korean government has taken measures to improve the air quality of the Greater Seoul Area since 2005. One of the major thrusts of its environmental policies has been to reduce the emission of particulate matters (PM) from diesel vehicles through the replacement of diesel buses with compressed natural gas (CNG) buses, installation of emission control devices such as diesel particulate filters (DPFs), and putting old diesel vehicles out of service. Our KIST research team has been focusing its efforts on characterizing traffic-related air pollution and investigating the effect of vehicle exhaust on air quality and public exposure levels in a variety of living environments. Our studies support the need and basic strategies of traffic-related environmental policies. After five years of research, we have developed a multi-functional mobile laboratory as an advanced monitoring tool. This work was supported by the Center of Environmentally Friendly Vehicles, a part of the Korean Ministry of Environment's Eco-STAR project.

Research Topics on Traffic-Related Air Pollution

Many researchers think that the contribution of vehicle exhaust to PM contamination of urban air is dominant in the Greater Seoul Area if fugitive emission sources are excluded [2]. However, it's very hard to evaluate the contribution of a specific air pollution source to air contamination because of many influencing factors. Results related to vehicular contribution to urban air pollution can vary significantly depending on the evaluation methods used, such as source-receptor modeling and emission inventory estimation, probably because of little understanding about real-world phenomena. Therefore, multi-directional and intensive research covering emission characteristics, transport phenomena from sources, and real-world exposure levels for health risk assessment should be carried out to fully understand traffic-related air pollution, as shown in Fig. 1. [3]

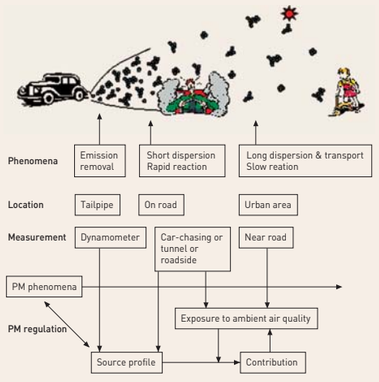

FIGURE 1. Block diagram of vehicle nanoparticle studies on ambient air quality. [3]

FIGURE 2. 2005 photo showing roadside monitoring of air pollution before development of a multi-functional mobile laboratory in 2009.

Our KIST team is conducting intensive research involving measurement of vehicular pollution at roadside and on-road locations, and during chase conditions, (Fig. 1) while collaborating with experts on engines and health risk assessment. Our team is the first in Korea to conduct this type of investigation. We are focusing on the monitoring of nanoparticles and black carbon (BC), as well as gaseous pollutants such as NO_x and CO, because they are not only associated with vehicles, but also with recent environmental issues such as public health and climate change [1, 4]. Black carbon is often referred to as soot or elemental carbon. PM_{10}, the mass concentration of particles <10 μm, has been measured at air quality monitoring stations and has, up to now, been one of the criterion of air quality standards, but it is not a proper indicator for evaluating vehicle exhaust because of the potentially significant impact from other emission sources, such as fugitive emissions, and its relatively low correlation with health risk compared to smaller particles.

Roadside Measurement

Emission characterization of vehicle exhaust has often been conducted in laboratories using an engine and chassis dynamometers. This type of analysis is mainly used to establish emission standards for regulation and to test new vehicle technologies. However, dynamometer measurement may not accurately reflect emissions under real-road driving conditions or take into account the vehicle conditions of an actual fleet [5, 6]. For these reasons, roadside measurement of air pollutants, in particular nanoparticles and black carbon, is useful for investigating the real-world emission characteristics of vehicle exhaust and to obtain exposure data on air pollutants affecting passengers walking along the road or people working or living near roads. For example, since the enactment of environmental regulation in 2004, the American city of Los Angeles is no longer constructing new schools within 500 ft (about 168 m) of freeways in order to protect the health of students [7].

Before the development of a multi-functional mobile laboratory, it was necessary for our monitoring team to protect aerosol instruments and gas analyzers for roadside monitoring with metal cabinets and to supply wall power using extended power cables, as shown in Fig. 2.

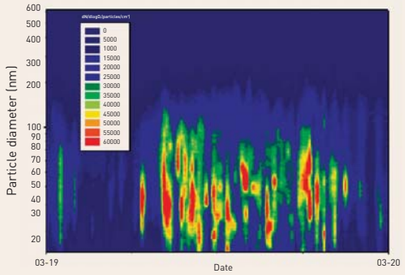

FIGURE 3. Diurnal variation of particle size distribution on March 19, 2005. Diameter is indicated on the vertical axis and particle concentration ($dN/dlogD_p$) is represented by color contours. [8]

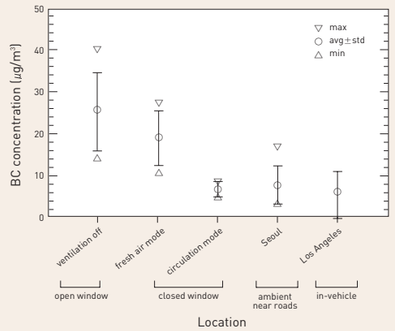

FIGURE 4. Comparison of black carbon exposure level measured in a vehicle and in ambient air. [3]

Figure 3 shows the diurnal variation of particle size distributions which were measured every five minutes at the roadside in front of Yonsei University at Shinchon-dong, Seodaemun-gu, Seoul, in 2005 [8]. Particle sizes ranged from 14 nm to 615 nm. The high concentration peaks of particles in the size range of 20 to 80 nm were observed very frequently, in particular between morning and evening rush hours. The exposure level of nanoparticles at the roadside fluctuated dramatically for short periods depending on the traffic situation and meteorological parameters.

Indoor air quality next to busy roads was found to be negatively affected through penetration of air pollutants so that indoor black carbon concentration was about half of that at the roadside. Air inside roadway tunnels was very contaminated by vehicle exhaust, especially at the tunnels exits; the black carbon exposure level inside tunnels was around three times higher than that at the roadside.

On-road Measurement

Although the distance between a roadside monitoring site and on-road vehicles is short, there might be dispersion and transformation of air pollutants during transport from a tailpipe to the sampling location. Therefore, on-road measurement is useful for characterizing the real emission phenomena of vehicle exhaust, particularly by following a target vehicle before and after the installation of emission control devices, such as DPF, as well as by examining in-vehicle exposure to normal drivers from vehicle exhaust, even without having a specific target vehicle ahead on the road.

BC concentrations, measured with a portable aethalometer placed on the passenger seat of a car driving on real roads in Seoul, were found to vary according to spatial location, time of day, and ventilation modes, as shown in Fig. 4. Average in-vehicle BC concentration under open vehicular window conditions was 25±10 $\mu g/m^3$, which was higher than the average BC concentration when the vehicle windows were closed (both in fresh air as well as circulation modes) and higher than the 24-hr average measured 200 m away from a road in Seoul and the in-vehicle concentration of Los Angeles under conditions of closed windows in a circulation mode [3].

Development of Mobile Laboratory

Traffic-related air pollution near roads is often found to have pollution "hot spots" characterized by significant spatial and temporal variations. Therefore, air pollution information obtained at fixed monitoring stations measured with wall-powered instruments having measurement time intervals of a few minutes is insufficient to explain traffic-related air pollution. A spatial distribution map of air contamination stemming from vehicle exhaust is needed to complement the data from stationary monitoring stations in order to be useful for detailed health risk assessment.

In 2009, we developed a multi-functional mobile laboratory with Grand STAREX to enable rapid monitoring of traffic-related air pollution near roads (Fig. 5). This project was conducted in collaboration with the Korea Institute of Machinery and Materials and the College of Medicine at Yonsei University. This mobile laboratory allows us to perform several important functions for monitoring air quality at either fixed locations or while driving. Emission measurements can be taken while following a target vehicle and animal exposure experiments can be conducted by exposing mice or rats to real vehicle exhaust. Typical air pollutants emitted from vehicles, such as NO_x, CO, hydrocarbons, can be measured. The number concentration of particles >5 nm, surface area concentration of particles deposited on a lung, size distribution of nanoparticles ranging from 5.6 to 560 nm, and particle-bound polycyclic aromatic hydrocarbons can be monitored using real-time instruments. As regards climate change issues, black carbon and CO_2 can also be measured in the mobile laboratory. Monitored air pollution data with averaging intervals of 1 sec~1 min can be logged in conjunction with meteorological data such as wind speed and direction, driving conditions such as vehicle speed, and geographical position like latitude and longitude.

Figure 6 shows one set of monitoring results obtained while using the mobile laboratory. These data show the spatial distribution of number concentration of particles >5 nm measured every second on the major roads of Nowon-gu, Seoul, in 2010, while driving in traffic flow [9]. The particle number concentration inside the KIST campus, which was the departure and arrival location, was as low as less than 20,000 particles/cm^3, a level also observed on major roads like Dongil Road but just for a brief time. Drivers would be exposed to severely contaminated air with a high particle number concentration greater than 200,000 particles/cm^3 four times per 1 hour if vehicular windows were open. The air pollution level on the roads fluctuated significantly depending on the traffic situation, type of vehicles traveling, and meteorological conditions.

Summary

For more than six years, our KIST research team has been conducting intensive research on traffic-related air pollution with a focus on nanoparticles and black carbon as well as standard air pollutants. Much of this research has involved multidisciplinary collaboration to understand the effect of vehicle exhaust on urban air quality and public health. We have looked at vehicular air pollution and compared exposure levels in various real environments such as at the roadside, within moving vehicles, inside roadway tunnels, and indoors next to busy roads. We found that air pollution exposure level on the roads can be about three times higher than at the roadside; therefore, it is highly recommended that drivers shut vehi-

FIGURE 5. Multi-functional mobile laboratory for detailed monitoring of traffic-related air pollution.

FIGURE 6. Spatial distribution of number concentration of particles larger than 5 nm measured with a mobile laboratory in Nowon-gu, Seoul, on October 5, 2010. [9]

cle windows and pedestrians avoid walking near busy roadways. Childcare facilities and adult health centers should be constructed as far as possible from busy roads to minimize adverse health effects. Long-term monitoring data of black carbon and CO_2 can be used to establish environmental policy for mitigating climate change.

Our research technology and achievements related to traffic-related air pollution have been exhibited several times at the International Exhibition on Environmental Technologies. Our next efforts will include making a detailed air pollution map of roadside and on-the-road locations for health risk assessment through regular monitoring of air pollution using the multi-functional mobile laboratory with its advanced real-time monitoring system. In addition, the mobile laboratory can be utilized even more extensively in the future to manage air pollution issues caused not only by vehicles, but also by construction of new buildings, exhaust of ships at ports, explosions or fires, and output from huge industrial complexes.

Vehicle exhaust is considered a major air pollution source in urban areas, particularly in mega-cities like Seoul.

NOTE

This article was drawn from our papers as follows:
Asian J. Atmos. Environ., 1-1, 1, 2007 [ref 3], and Particle and Aerosol Res., 7, 21, 2011 [ref 9]

REFERENCES

1. M.C. Power, M.G. Weisskopf, S.E. Alexeeff, B.A. Coull, A. Spiro III, J. Schwartz, Environ. Health Persp., doi: 10.1289/ehp.1002767, 2010
2. H.S. Lee, C.-M. Kang, B.-W. Kang, S.-K. Lee, J. Korean Soc. Atom. Environ., 21, 329, 2005.
3. G.-N. Bae, S.-B. Lee, S.-M. Park, Asian J. Atmos. Environ., 1-1, 1, 2007.
4. V. Ramanathan, G. Carmichael, Nature Geoscience, 1, 221, 2008.
5. N.T. Kim Oanh, M. Martel, P. Pongkiatkul, R. Berkowicz, Atmos. Res., 89, 223, 2008.
6. D.B. Kittelson, W.F. Watts, J.P. Johnson, J. Aerosol Sci., 37, 913, 2006.
7. R.S. Green, S. Smorodinsky, J.J. Kim, R. McLaughlin, B. Ostro, Environ. Health Persp., 112, 61, 2004.
8. G.-N. Bae, S. Huh, S.-B. Lee, M. An, D. Park, J. Hwang, Particle and Aerosol Res., 3, 29, 2007.
9. S.-B. Lee, D.-H. Lee, S.J. Lee, H.C. Jin, G.-N. Bae, Particle and Aerosol Res., 7, 21, 2011.

KIST's Role in the Expansion of Scientific Technology ODA

Hea Jin Lim
Senior Researcher, Econimics Ph.D
Technology Policy Research Institute
•
hjlim@kist.re.kr

'Give a man a fish and he will eat for a day; teach a man to fish and he will eat for a lifetime'

Developing countries are becoming more open to Official Development Assistance (ODA) related to scientific technology and are especially interested in the technological expertise and scientific technology development experiences of Korea. There are various Korean-style ODA models which have been classified as the KIST, KAIST, Daedeok Innopolis, and Techno-Park styles, as well as others, according to their specific features (2011, Ki Kook Kim). In applying these models to other countries however, more efficient support and contributions can be offered if the model is tailored to the unique conditions inherent in each developing country, such as technology capability, education, income level and needs.

In 2010, a number of important leaders visited KIST to request assistance in establishing research laboratories as well as learn from our management experiences. These leaders included the President of Ecuador (Sept 10), Foreign Secretary (Sep 16), and Science and Technology Minister (Nov 2) of Costa Rica, Science and Technology Minister of Ethiopia (Sep 14) and Education and Science Minister of Zimbabwe (May 27). KIST particularly attracted their attention because it was initially established in 1966 with the financial support and assistance of the United States Agency for International Development (USAID) and since then has attained world-class expertise in research and played a key role in the success of Korea's economy. As a result of this impressive history, KIST is regarded as a successful management model, one which is now in high demand in developing countries.

Since its establishment, KIST has spawned 12 public research institutes, proving that it has the best background in scientific technology ODA in Korea. Moreover, KIST has actively promoted ODA as a result of the broad experience it has gained through the establishment of branch institutes and overseas laboratories as well as the development of an extensive infrastructure both in and outside the country. KIST is supporting both the establishment of similar research institutions in other countries based on the developing country's needs, and educational facilities focused on advanced scientific technology which are required in order to effectively run the research institutions. ODA projects that KIST has promoted are shown below

OVERVIEW OF KIST'S ODA PROJECTS

Organization	Description
International R&D Academy (IRDA)	• International training program for technical professionals from developing countries • Opened in 2001 and currently has approximately 100 students enrolled in master's and doctoral programs
Korea International Cooperation Agency (KOICA) Project	• Supported the establishment and operation of Korea-Vietnam science and technology coordination center ('00-'01, $2,880,000) • Project involving the transfer of development experience between Korea and Vietnam ('10.6-'11.12, $1,200,000, in association with Hankyung University) • Established an energy environment research center in Indonesia ('10.6-'12.12, $2,500,000) • Conducted research on antipollution measures for the Yellow Sea of China ('08-'10, $500,000)
Korea International Cooperation Agency (KOICA) Training project	• Provides annual training in support of the developing country's sustainable development by sharing experience related to enviropolicies and technology development • Korea-Japan joint training on air and water quality
Ministry of Science and Education	• Korea-Mongolia science and technology coordination center ('02-in progress) KIST • VAST (Vietnam Academy of Science and Technology) administration training ('09)

KIST's ODA model includes five main areas including ❶ establishment of research infrastructure, ❷ establishment of education programs to train advanced researchers, ❸ provision of technical support, ❹ establishment of research networks, and ❺ consulting on policy issues associated with the implementation of Korean-style scientific technology ODA models.

KIST is currently establishing a science education center in Mongolia and scientific technology laboratories in Southeast Asia (Cambodia, Laos) to support the establishment of a research infrastructure for the region. KIST is also initiating various education programs for advanced training of scientific technology experts based on its considerable experience in operating the IRDA program. Specifically, KIST is promoting a special master's program for science students in developing countries such as Cambodia, as well as a training program for senior science and technology administrators. Another strategy of KIST is to establish networks and encourage education programs as cooperative projects with developing countries and to assist them in establishing future strategies for S&T development. As part of this initiative, KIST held a meeting earlier in 2011 in Korea of science and technology diplomats from developing countries and is planning to hold a scientific technology ODA forum in October of this year. KIST is in a position to lead the development of multi-convergence ODA programs and provide valuable technical support for this initiative. As the only existing national research institute that performs R&D integration and convergence, KIST has a superior capability in convergence technology related to 'the global public goods through ODA'. In addition, it aspires to play a key role in science and technology policy consulting to reinforce future science and technology cooperation with developing countries through working together on global issues. Though KIST was involved in the establishment of Indonesia's enviropolicies in 2010, more such activities are needed.

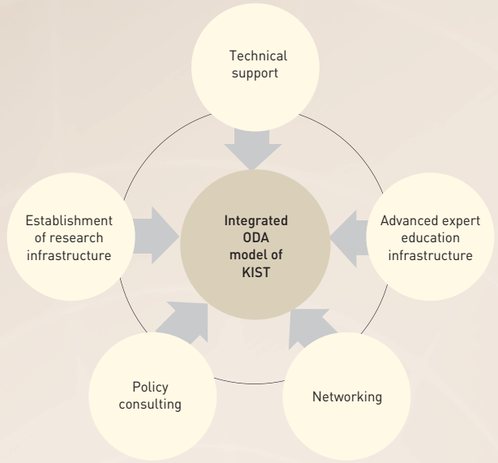

KIST is committed to reinforcing its capability in ODA by developing the contents related to its ODA experience, and expanding ODA expert education and an ODA department in order to implement the initiatives stated above.

KIST is committed to reinforcing its capability in ODA by developing the contents related to its ODA experience, and expanding ODA expert education and an ODA department in order to implement the initiatives stated above. To accomplish this, KIST will promote and use its ODA advisory committee, organized in 2011, to systematize ODA projects and also develop a variety of supporting systems. As an example, although the Global KIST Project, an international cooperation research program, consists of a total of 20 projects, only 4 of them (1 natural substance, 1 water quality and 2 energy projects) are related to developing countries and supported with funds for ODA project development; thus, there is considerable potential to increase the number of such projects. Through such untiring efforts, KIST will firmly establish an ODA model that works, and thus be able to pass down not the 'myth of S&T development', but 'an actual history' of success to foreigners who visit Korea to learn from our example.

The Enhancement of Mature Vessel Formation and Cardiac Function in Infarcted Hearts Using Dual Growth Factor Delivery with Self-assembling Peptides

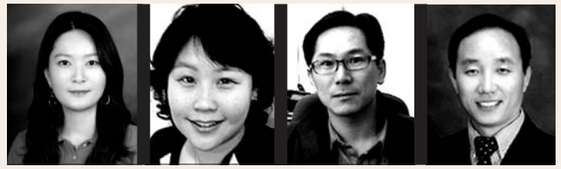

Ji Hyun Kim, Youngmee Jung, Sang-Heon Kim, Soo Hyun Kim

Biomedical Research Institute, Center for Biomaterials

•

soohkim@kist.re.kr

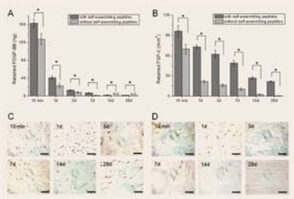

FIGURE 1. Sustained delivery of growth factors by self-assembling peptides. Injection of self-assembling peptides can provide sustained delivery of PDGF-BB and FGF-2 for 1 month. Without self-assembling peptides, few or no growth factors are detected at 14 days and 28 days in the injected site. (A) Retained PDGF-BB at injected sites analyzed with human PDGF-BB ELISA, *$p < 0.05$. (B) Retained FGF-2 at injected sites. After staining with anti-FGF basic antibody, staining for FGF-2 was counted in 3 different fields. N.D. = not detected. *$p < 0.05$. (C) and (D) Immunohistochemistry of FGF-2 injected with/without self-assembling peptides, respectively. Scale bars: 50 μm (x400).

Congestive heart failure is a leading cause of morbidity and mortality in many countries [1, 2]. The dominant cause of heart failure, including myocardial infarction (MI), is regional damage or death of heart muscle tissue due to coronary artery disease and ischemia that leads to cardiomyocyte necrosis and apoptosis [3, 4]. Therefore, to prevent fibrosis in the myocardium it is crucial to prevent cardiomyocyte apoptosis and maintain an accurate blood flow to the infarcted area.

Several approaches in cardiac tissue engineering have been investigated for the treatment of MI [2, 5, 6]. This includes various kinds of angiogenic factors such as vascular endothelial growth factor (VEGF), epidermal growth factor (EGF), fibroblast growth factor (FGF), and platelet-derived growth factor (PDGF) which have been studied for their effects in cardiac repair. These growth factors were directly injected into myocardium or sometimes delivered with various natural matrices such as gelatin, alginate, or synthetic materials including self-assembling peptides [4, 6-9]. In animal experiments, these growth factors were shown to promote endothelial cell (EC) growth in areas of MI. However, long-term animal studies and large randomized clinical trials have indicated that these strategies are not beneficial in humans [10-12]. For example, the delivery of a single angiogenic factor targeting ECs is still unable to cause the formation of stable blood vessels.

To establish stable and functional vascular networks for treatment of ischemic tissues, complex angiogenic and arteriogenic processes that stimulate ECs and vascular smooth muscle cells (VSMCs) are needed because vessels are composed mainly of ECs and VSMCs [13-15]. Recently, studies using several growth factors have been carried out, and it appears that the choice of optimal growth factors is a crucial issue for successful therapy [10, 13, 15-17]. *Cao Y et al.* showed stable vessel formation in various tissues with angiogenic and arteriogenic growth factors [14, 16, 18-20]. In Cao Y's study, they were able to form a stable vessel network with ECs and VSMCs by combining, among various angiogenic and arteriogenic factors, FGF-2 and PDGF-BB. Generally, FGF-2 stimulates angiogenesis involving ECs [21]. PDGF-BB acts mainly on vascular mural cells including pericytes and VSMCs involved in vascular network maturation and remodeling [4, 14, 22, 23].

Various hydrogels such as gelatin, alginate, collagen, fibrin, and self-assembling peptides nanofiber hydrogel are being examined for treatment of MI [2, 5, 6]. These hydrogels act as biomaterial scaffolds and sometimes, injectable scaffolds to deliver cells or growth factors. In particular, synthetic self-assembling peptides are promising candidates for biomaterials in tissue engineering and regenerative medicine [24-27]. Since they are composed of synthetic amino acids, unlike other natural hydrogels derived from animals, they can be easily designed and modified in a variety of ways, and it is possible to control degradation rates with non-immunogenicity. This injectable biodegradable material forms fibers (5 to 10 nm) and assembles into a 3-dimensional (3D) scaffold at physiological pH and osmolality. The scaffolds closely mimic the porosity and gross structure of extracellular matrices, allowing cells to reside and migrate in the microenvironment, and supporting cell attachment and differentiation of a variety of cells [27-31].

In our study, dual growth factors and self-assembling peptides were applied to an MI animal model. The goal was to achieve cardiac function recovery by preventing cardiomyocyte loss and establishing stable and functional vessels. Both angiogenic (FGF-2) and arteriogenic (PDGF-BB) factors were combined, thus targeting ECs and VSMCs [16]. By injecting dual growth factors with self-assembling peptides (RADA16-II), we sought to provide a local 3D microenvironment in the myocardium, and we expected to recruit both ECs and SMCs that promoted vascularization and prevented cardiac fibrosis, as well as providing long-term delivery of dual growth factors [4, 28, 32].

First of all, sustained growth factor delivery of self-assembling peptides injected into infarcted myocardium was estimated. Local sustained delivery of therapeutic proteins is important to cardioprotection because it can prevent rapid diffusion of proteins from the injected site [33-35]. In this study, a sustained growth factor delivery test was performed in a mouse hind limb model. With self-assembling peptides, growth factors remained at the injected site after 28 days (Fig. 1). Therefore, remaining growth factors can be expected to cause prolonged activation of the injected sites. Actually, the precise mechanism of the sustained release of proteins is not yet understood. RADA16-II, which was used in this study, has no specific binding motif, so adsorption of growth factors on RADA16-II by non-covalent interaction with the amphiphilic RADA16-II is the most plausible explanation suggested by *Lee RT et al* [35]. In our system, it is assumed that adsorption by the structural properties of RADA16-II enables PDGF-BB and FGF-2 delivery to be sustained.

To establish functional stable vessels, dual growth factor along with self-assembling peptides was applied to the area of a MI. After coronary artery ligation in rats, growth factors (PDGF-BB and

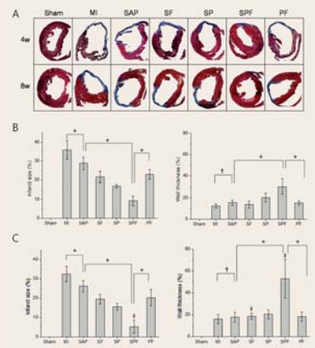

FIGURE 2. Infarct size and wall thickness of infarcted hearts. Intramyocardial self-assembling peptides along with PDGF-BB and FGF-2 injection reduce infract size and increase wall thickness 4 and 8 weeks after myocardial infarction. (A) Representative pictures of left ventricles from each group after Masson's Trichrome staining. (B) and (C) Infarct size and wall thickness as percentages at 4 weeks and 8 weeks, respectively. Infarct size is calculated as the ratio of infarcted to non-infarcted area of the left ventricle. Wall thickness is calculated as the ratio of the thickness of the infarcted wall to that of the non-infarcted septal wall determined with an image analysis system. *$p < 0.05$, †$p > 0.05$, ‡$p < 0.05$ for 4 weeks versus 8 weeks.

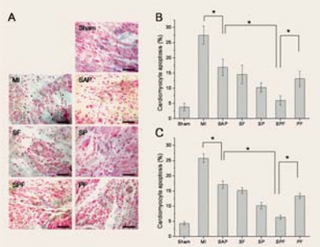

FIGURE 3. Cardiomyoyte apoptosis of infarcted hearts. Injection of PDGF-BB and FGF-2 with self-assembling peptides decreases cardiomyocyte apoptosis 4 and 8 weeks after infarction. (A) Immunohistochemistry of TUNEL staining in the border zone at 4 weeks. Live cell: pink. Apoptotic cells: dark blue. Scale bars: 50 μm (x400). (B) and (C) The ratio of TUNEL-positive to total nuclei (expressed as a %) was quantified at 4 weeks and 8 weeks, respectively. *p $<$ 0.05.

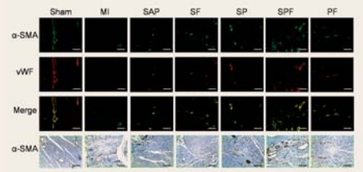

FIGURE 4. Representative immunostaining of endothelial cells (ECs) and vascular smooth muscle cells (VSMCs) of each group 4 weeks after infarction. In immunofluorescence, ECs are stained with von Willebrand factor (vWF, red) and VSMCs are stained with α-smooth muscle actin (α-SMC, green). In immunohistochemistry, VSMCs are stained with α-smooth muscle actin (α-SMC). Scale bars: 100 μm (x200).

FGF-2) with self-assembling peptides were injected. We studied 7 groups of rats (n = 6 in each group): sham, MI + sucrose (MI), MI + self-assembling peptides (SAP), MI + self-assembling peptides and FGF-2 (SF), MI + self-assembling peptides and PDGF-BB (SP), MI + self-assembling peptides, PDGF-BB, and FGF-2 (SPF), MI + PDGF-BB and FGF-2 (PF). Hearts were harvested at 4 and 8 weeks for functional and histological analysis. Based on the results of Masson's trichrome staining, infarct size and wall thickness were calculated by an image analysis system (Fig. 2). The infarct size of the SPF group was 4 times lower than that of the MI group. Wall thickness for SPF was 3.33 times higher than that of the MI groups 8 weeks after infarction. Injection of dual growth factors with self-assembling peptides was the most effective in preventing cardiomyocyte apoptosis (Fig. 3). To validate the angiogenic and arteriogenic effects of dual growth factors with self-assembling peptides, the capillary and arterial density and maturation index of each group were analyzed, and in the case of SPF, there were no differences in compared sham (Fig. 4 and 5). To study improvements in cardiac function after therapy using combined factors, functional analysis was performed. SPF was the most effective treatment for improving cardiac function (Fig. 6).

Injected self-assembling peptides in infarcted regions rapidly form nanofibers (5 ~ 10 nm) and assemble into 3D microenvironments that are similar to extracellular matrix [29, 30, 32]. These microenvironments allow various cells to infiltrate easily and to attach and survive long-term [24, 28, 32]. Our study showed that injecting self-assembling peptides into myocardium leads to cardiomyocyte protection, fibrosis prevention, and matured vessel formation. These results imply (i) that injected self-assembling peptides can create microenvironments; and (ii) that recruited ECs and VSMCs within microenvironments form stable and long-lasting vascular networks.

To establish a stable and functional vessel network, the selection of appropriate growth factors is important [10, 13, 15-17]. To stimulate angiogenesis, many current studies have used dual growth factors based on VEGF with FGF-2, PDGF-BB, angiopoietin-1 or keratinocyte growth factor, all of which have showed improved microvessel density in short-term in vivo experiments [14, 36, 37]. Generally, FGF-2 has been shown to stimulate proliferation of various cells, including ECs and SMCs, that are involved in regulation of cell survival and migration [21, 38]. In our study, we formed a stable vessel network by combining FGF-2, which is related to ECs, and PDGF-BB, which is related to VSMCs. Interestingly, our data show that a specific combination of PDGF-BB and FGF-2 synergistically induces and establishes a functional and stable vascular network, one that remains stable for more than 8 weeks, even after depletion of the growth factors.

A possible mechanism of the angiogenic synergism between PDGF-BB and FGF-2 can be explained by the co-expression of PDGFR-α, PDGFR-β, and FGFRs [14, 16, 18, 20]. PDGF-BB interacts with both homodimeric and heterodimeric PDGFR-α and PDGFR-β. PDGF-β, expressed on VSMCs plays a crucial role in vessel stability and maturation, and PDGF-α expressed on ECs is related to angiogenesis. FGF-2 primarily acts on FGFRs expressed on ECs to promote angiogenesis and also up-regulate expression levels of PDGFR-α in ECs and PDGFR-β in VSMCs. These signaling pathways are co-activated simultaneously, which leads to an angiogenic synergism and vessel stability [16, 18]. To improve synergism, a combination of various growth factors and their dose dependence would be required.

Our results demonstrated that angiogenic synergism increased when dual growth factors were combined with self-assembling peptides. Synergistic effects were observed in capillary and arterial density (~2 and 4 times, respectively). It is thought that the 3D microenvironment created by injecting self-assembling peptides plays a role in preventing cardiac fibrosis and in recruiting cardiomyocytes. Recruited ECs and VSMCs and long-term delivered dual growth factors form well-organized vascular structures within the myocardium. Sufficient blood supplied by stable matured vessels into the myocardium promotes vascular cell and cardiomyocyte survival, and also restores cardiac function. Here, special attention should be paid to the cardiac function restoration of the SPF group. Although the other groups showed histologic improvements, only dual growth factors in combination with self-assembling peptides significantly improved all 4 hemodynamic parameters related to cardiac function. To the best of our knowledge, the delivery of angiogenic and arteriogenic factors in combination with self-assembling peptides to a myocardial infarction has not previously been reported.

The combined therapy of dual growth factors along with self-assembling peptides protects the myocardium by preventing cardiomyocyte apoptosis and establishing stable vessels, and leads to recovery of cardiac function. Self-assembling peptides provide an injectable 3D microenvironment for recruiting ECs and VSMCs and preventing cardiac fibrosis, and play a role in the sustained delivery of growth factors. A combination of FGF-2 and PDGF-BB, which are therapeutically beneficial, form stable and functional vessels with angiogenic synergism. Moreover, because the self-assembling peptides are injectable, biodegradable, synthetic, and non-immunogenic, they are almost ready to be applied in clinical research. Based on these results, the combination of dual growth factors with self-assembling peptides can provide cardiac protection of potential therapeutic importance and is a good subject for future studies examining combinatorial factors to treat acute myocardial infarction.

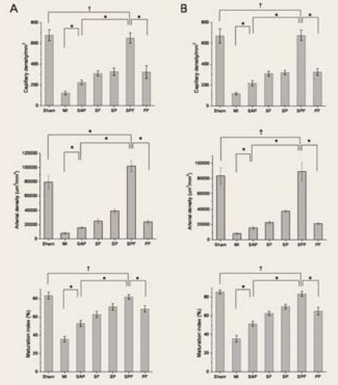

FIGURE 5. Capillary density, arterial density and maturation index. Injection of PDGF-BB and FGF-2 along with self-assembling peptides improves capillary and arterial density and the maturation index. Quantification of capillary density was done by counting vWF-positive vessels and arterial density by measuring the area of α-SMC- positive vessels. Quantification of the maturation index was done by comparing the percentage of α-SMA-positive vessels to the total number of vessels. (A) and (B) 4 and 8 weeks after infarction, respectively. *p $<$ 0.05, $^{+}$p $>$ 0.05.

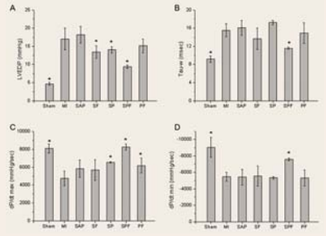

FIGURE 6. Cardiac function analysis. Injection of PDGF-BB and FGF-2 along with self-assembling peptides improves cardiac function 4 weeks after infarction. (A) LVEDP indicates left ventricular end diastolic pressure. (B) Tau-w, Tau Weiss parameter. (C) dP/dt max. (D) dP/dt min. *$p < 0.05$ versus MI.

REFERENCES

1. Jessup, M. and S. Brozena, Heart failure. N Engl J Med, 2003. **348**(20): p. 2007-18.
2. Jawad, H., et al., *Myocardial tissue engineering: a review.* J Tissue Eng Regen Med, 2007. **1**(5): p. 327-42.
3. Anversa, P., *Myocyte death in the pathological heart.* Circ Res, 2000. **86**(2): p. 121-4.
4. Hsieh, P.C.H., et al., *Controlled delivery of PDGF-BB for myocardial protection using injectable self-assembling peptide nanofibers.* Journal of Clinical Investigation, 2006. **116**(1): p. 237-248.
5. Eschenhagen, T. and W.H. Zimmermann, *Engineering myocardial tissue.* Circ Res, 2005. **97**(12): p. 1220-31.
6. Christman, K.L. and R.J. Lee, *Biomaterials for the treatment of myocardial infarction.* J Am Coll Cardiol, 2006. **48**(5): p. 907-13.
7. Hao, X., et al., *Angiogenic effects of sequential release of VEGF-A165 and PDGF-BB with alginate hydrogels after myocardial infarction.* Cardiovasc Res, 2007. **75**(1): p. 178-85.
8. Shao, Z.Q., et al., *Effects of intramyocardial administration of slow-release basic fibroblast growth factor on angiogenesis and ventricular remodeling in a rat infarct model.* Circ J, 2006. **70**(4): p. 471-7.
9. Zisch, A.H., M.P. Lutolf, and J.A. Hubbell, *Biopolymeric delivery matrices for angiogenic growth factors.* Cardiovasc Pathol, 2003. **12**(6): p. 295-310.
10. Simons, M., *Angiogenesis: where do we stand now?* Circulation, 2005. **111**(12): p. 1556-66.
11. Khurana, R., et al., *Role of angiogenesis in cardiovascular disease: a critical appraisal.* Circulation, 2005. **112**(12): p. 1813-24.
12. Annex, B.H. and M. Simons, *Growth factor-induced therapeutic angiogenesis in the heart: protein therapy.* Cardiovasc Res, 2005. **65**(3): p. 649-55.
13. Carmeliet, P., *Mechanisms of angiogenesis and arteriogenesis.* Nat Med, 2000. **6**(4): p. 389-95.
14. Cao, R., et al., *Angiogenic synergism, vascular stability and improvement of hind-limb ischemia by a combination of PDGF-BB and FGF-2.* Nat Med, 2003. **9**(5): p. 604-13.
15. Semenza, G.L., *Vasculogenesis, angiogenesis, and arteriogenesis: mechanisms of blood vessel formation and remodeling.* J Cell Biochem, 2007. **102**(4): p. 840-7.
16. Lu, H., et al., *Combinatorial protein therapy of angiogenic and arteriogenic factors remarkably improves collaterogenesis and cardiac function in pigs.* Proc Natl Acad Sci U S A, 2007. **104**(29): p. 12140-5.
17. Simons, M., et al., *Clinical trials in coronary angiogenesis: issues, problems, consensus: An expert panel summary.* Circulation, 2000. **102**(11): p. E73-86.
18. Zhang, J., et al., *Differential roles of PDGFR-alpha and PDGFR-beta in angiogenesis and vessel stability.* Faseb Journal, 2009. **23**(1): p. 153-63.
19. Nissen, L.J., et al., *Angiogenic factors FGF2 and PDGF-BB synergistically promote murine tumor neovascularization and metastasis.* Journal of Clinical Investigation, 2007. **117**(10): p. 2766-77.
20. Cao, Y., R. Cao, and E.M. Hedlund, *R Regulation of tumor angiogenesis and metastasis by FGF and PDGF signaling pathways.* J Mol Med, 2008. **86**(7): p. 785-9.
21. Ornitz, D.M. and N. Itoh, *Fibroblast growth factors.* Genome Biol, 2001. **2**(3): p. REVIEWS3005.
22. Hsieh, P.C., et al., *Local controlled intramyocardial delivery of platelet-derived growth factor improves postinfarction ventricular function without pulmonary toxicity.* Circulation, 2006. **114**(7): p. 637-44.
23. Lindahl, P., et al., *Pericyte loss and microaneurysm formation in PDGF-B-deficient mice.* Science, 1997. **277**(5323): p. 242-5.
24. Davis, M.E., et al., *Custom design of the cardiac microenvironment with biomaterials.* Circ Res, 2005. **97**(1): p. 8-15.
25. Genove, E., et al., *The effect of functionalized self-assembling peptide scaffolds on human aortic endothelial cell function.* Biomaterials, 2005. **26**(16): p. 3341-51.
26. Gelain, F., A. Horii, and S. Zhang, *Designer self-assembling peptide scaffolds for 3-d tissue cell cultures and regenerative medicine.* Macromol Biosci, 2007. **7**(5): p. 544-51.
27. Horii, A., et al., *Biological designer self-assembling peptide nanofiber scaffolds significantly enhance osteoblast proliferation, differentiation and 3-D migration.* PLoS One, 2007. **2**(2): p. e190.
28. Narmoneva, D.A., et al., Self-assembling short oligopeptides and the promotion of angiogenesis. Biomaterials, 2005. **26**(23): p. 4837-46.
29. Zhao, X.J. and S.G. Zhang, *Fabrication of molecular materials using peptide construction motifs.* Trends in Biotechnology, 2004. **22**(9): p. 470-476.
30. Zhang, S.G., *Fabrication of novel biomaterials through molecular self-assembly.* Nature Biotechnology, 2003. **21**(10): p. 1171-1178.
31. Ellis-Behnke, R.G., et al., *Nano neuro knitting: peptide nanofiber scaffold for brain repair and axon regeneration with functional return of vision.* Proc Natl Acad Sci U S A, 2006. **103**(13): p. 5054-9.
32. Davis, M.E., et al., *Injectable self-assembling peptide nanofibers create intramyocardial microenvironments for endothelial cells.* Circulation, 2005. **111**(4): p. 442-50.
33. Carmeliet, P. and E.M. Conway, *Growing better blood vessels. Nature Biotechnology,* 2001. **19**(11): p. 1019-20.
34. Ozawa, C.R., et al., *Microenvironmental VEGF concentration, not total dose, determines a threshold between normal and aberrant angiogenesis.* Journal of Clinical Investigation, 2004. **113**(4): p. 516-27.
35. Segers, V.F.M. and R.T. Lee, *Local delivery of proteins and the use of self-assembling peptides.* Drug Discovery Today, 2007. **12**(13-14): p. 561-568.
36. Peattie, R.A., et al., *Dual growth factor-induced angiogenesis in vivo using hyaluronan hydrogel implants.* Biomaterials, 2006. **27**(9): p. 1868-75.
37. Elia, R., et al., *Stimulation of in vivo angiogenesis by in situ crosslinked, dual growth factor-loaded, glycosaminoglycan hydrogels.* Biomaterials, 2010. **31**(17): p. 4630-8.
38. Detillieux, K.A., et al., *Biological activities of fibroblast growth factor-2 in the adult myocardium.* Cardiovascular research, 2003. **57**(1): p. 8-19.

Human-Centered Coexistent Space for the Convergence of Humans, Artifacts, and the Virtual World

Bum-Jae You, Ph. D.
Director, Center of Human-Centered Interaction for Coexistence
•
ybi@kist.re.kr

New innovative technologies are bringing about lifestyle changes and cultural shifts as well as major impacts on the world economy and social relationships. For example, the internet has enabled a PC to serve as a gateway for information and a means to develop and maintain social relationships, while smart mobile phones, tablet PCs and wireless network have made network connectivity available from almost any location. Human-centered science and technology have become more important and require more attention from researchers, engineers, and technology users as people seek ways to make their lives more comfortable and convenient.

Futurologists predict the boundaries between human and machine or between reality and virtual reality will collapse by 2020, and the intelligence of machines will gradually begin to transcend human intelligence by 2030. The era of trans-human replacement of human body parts with bionics will come by 2040. These predictions are based on human-centered technology development involving the fusion of NBIC (Nano, Bio, Information, and Cognitive) technologies. In particular, information and communication technology in conjunction with software technology will provide the basis for technology fusion and innovation.

In the 2009 movie *Surrogates*, future society in 2017 is depicted as one in which everyone lives their lives through their own surrogate robots. People go to work and school not by being physically present, but through these surrogates which can be made to move and respond just as their individual controllers would through bionic human interfaces. This vision reflects a society where individuals simply sit down and control their personal agents directly, without acually going to work or school, but where outcomes are the same as if they were physically there. In this way, it is possible to avoid the risk of injury or illness, and maintain a "perfect" appearance without aging or cosmetic surgery. The scene is similar to the movie, *Avatar*. In that film, although Jake Sully is disabled in real life, he can be active and experience adventures through his avatar, connected to his brain through an advanced bionic human interface.

If robots can function perfectly as humans in the future, what would happen? Scenes from films based on this concept are clearly fictional, but researchers and experts who study Brain Machine Interface say that such scenarios are quite feasible. Indeed, is it possible to develop surrogate robots, avatars, and virtual worlds similar to the realities represented in these films? One can imagine a new type of world, as shown in movies such as *Matrix*, *Surrogates*, or *Avatar*, in which a human being can experience a virtual world as a real world and a remote avatar as him/herself.

Human-Centered Coexistent Space

Three worlds are integral to daily life:the real world, virtual world, and remote world, as shown in Fig. 1. The real world is the space where we are physically present, such as the home or office. In this world there are many artifacts like networked printers, PCs, service robots, TVs, home appliances, prosthetics, motorized video cameras, etc. The virtual world refers to the cyberspace of computer systems such as those provided by computer games, PC user environments, cyber second lives, social network spaces, etc. Finally, the remote world physically exists, but one cannot be there. For example, one cannot be in New York at this instant if you are living in Seoul. In the remote world there are also many artifacts as in the real world.

Human-centered coexistent space is defined as the space where one can experience the virtual and remote worlds as if they were the real world. Through various human-centered solutions for coexistence, it will be possible to interact with the virtual world and remote world as the real world. It is expected that human-centered coexistent space will form the basis of future daily life by connecting human beings, artifacts, virtual worlds, and remote worlds.

Large amounts of information will be exchanged rapidly and consistently in coexistent space for natural interaction and mutual association between humans and artifacts, humans and the virtual world, humans and the remote world, as well as between one human and another. It will be necessary to develop many advanced natural human interfaces for bi-directional transfer of human intention, real sensation (seeing, listening, touching, smelling, tasting, and movement) and emotion. Information at billions of bits per second will be delivered to the human sense organs over the network, and it will even be possible to evaluate physical and emotional well-being.

Core Technologies

Three major technologies are required to develop coexistent space. First is a core technology that enables the coexistence of human and intelligent machines in real and

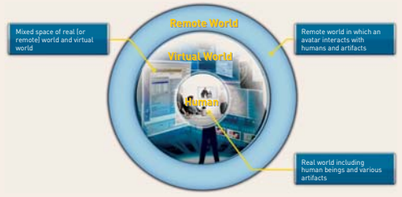

FIGURE 1. Human-Centered Coexistent Space

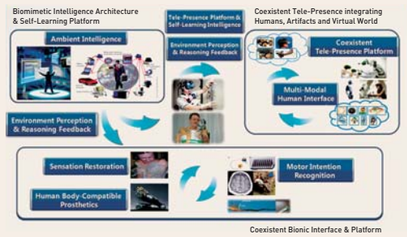

FIGURE 2. Coexistence of Humans and Intelligent Machines

remote worlds. It includes the development of multi-modal human interface, tele-presence, bionic human interface, and intelligence for learning human behaviors and sensation, as shown in Fig. 2. The purpose of these systems is to transfer human intention into artifacts in the real world, virtual world and remote world and to transmit real sensation back to the human. When this is achieved, humans can handle and feel objects in the real world, virtual world, and remote world.

A second core technology involves overcoming spatial and time constraints in the real world to enable the coexistence of human and virtual worlds. It includes technologies for constructing three-dimensional human avatars and mirror worlds that can handle objects interactively, augmenting the mirror world with a real (or remote) world, and allowing interaction between users and the mirror world, as shown in Fig. 3. The mirror world is a mixture of the real (or remote) world and the virtual world and is a space in which a human avatar can navigate in lieu of humans. Multiple users can meet to collaborate or interact in the mirror world.

The third core technology enables emotional interaction and innovative interaction forcoexistence. People can exchange social emotions and information with artifacts in real, virtual and remote worlds through innovative means like human body communication, as shown in Fig. 4. Social emotion can be detected by bio-signals from the human body or other visible clues which signal a change of emotions. In this way, emotional interaction with artifacts or other worlds will become possible.

Future Life

So how will the convergence of humans and artifacts in virtual and remote worlds shape the future of society? Humans will exchange intentions, feelings, and emotions with intelligent machines, virtual worlds and remote worlds while humans can interact with each other through the proposed human-centered coexistent space.

Human-centered coexistent space will provide alternative solutions for social networking and daily life. Individuals in several locations will be able to meet together at a place in coexistent space and share the same experience through the mirror world. This coexistent space may help reduce air pollution and travel costs by reducing traffic, an important consideration as societies look for ways to become more environmentally friendly. In addition, users can enter into the operating system of a computer and work easily by handling the information inside of the machine.

In an aging society, remote medical examination by doctors or nurses will be possible through live images, sounds, and direct touch of sore spots in the human body. Coexistent space will make medical examinations more precise and expand the capacity of medical services since the travel distance between doctor and patient can be eliminated. An additional advantage is that an elderly individual who cannot move arms or hands can control and manipulate home appliances through a coexistent interface based on sensation. A defective part of a human body can be replaced with wearable computers or human-like prosthetics providing real-time control and sensation.

Coexistent space also makes it possible to care for aging parents and other elderly dependents at long distance. One can watch, guide, and help parents without being at the same location. It is also expected that telecommuting, working at home for a company, will become increasingly popular in the future as a person at home can control a fully responsive avatar that is able to collaborate with other staff at the workplace.

In the future it will also be possible to recognize a person's emotional state by using a variety of physiological signals during conversation, leading to diagnosis of illness and ability to treat through psychotherapy and relaxation techniques, all in coexistent space. Furthermore, new media services to understand patients will be realized using real-time emotional information.

Supporting the Global Frontier Program

In August 2010, a Global Frontier Program was launched by the KoreanMinistry of Education, Science and Technology to develop core technologies for human-centered coexistent interaction. Funding has been earmarked for nine years. This program is aiming to develop basic core technologies beyond the limitations of conventional technologies and to establish a world-leading research center based on the "4G" philosophy of the Global Frontier Program: Ground Breaking, Group Approach, Global R&D, Green & Sustainability.

The Center of Human-Centered Interaction for Coexistence, CHIC for short,was founded for encouraging and managing innovative research to realize the new concept of coexistent space that did not previously exist. KIST's Dr. Bum-Jae You, who developed the world's first network-based humanoid robot *MAHRU* in 2005, is leading the whole project. Research teams at the Korea Institute of Science and Technology, Gwangju Institute of Science and Technology, Hanyang University, Sangmyung University, Korea Advanced Institute of Science and Technology, POSTECH, Samsung Advanced Institute of Technology, and Electronics and Telecommunications Research Institute in Korea, are all involved in the effort. KIST's specific contribution has been the establishment of the Interaction and Robotics Research Center to support MEST's Global Frontier Program and to collaborate closely with CHIC.

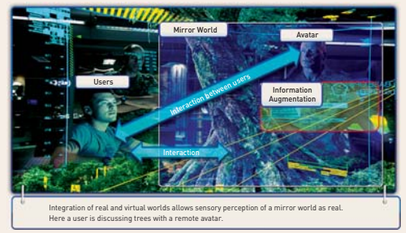

FIGURE 3. Coexistence of Humans and the Virtual World

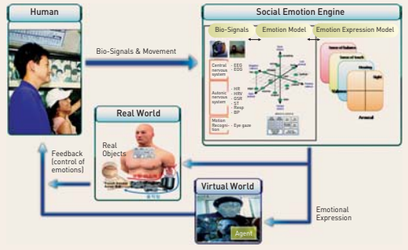

FIGURE 4. Emotional Interaction Framework for Coexistence

Binding of fluorophores to proteins depends on the cellular environment

Yun Kyung Kim
Brain Science Institute Center for Neuro-Medicine
•
yunkyungkim@kist.re.kr

The main focus of this article is on the identification of small-molecule targets in living cells. Identifying small-molecule targets is the most challenging part of chemical genetics. A major difficulty lies in that conventional target-identification methods require serious perturbation of the native cell environment, which is crucial for small-molecule localization and activity. Accordingly, only some targets isolated from in vitro assays have shown selective binding to the same molecule in living cells. Here, we show this limitation of in vitro target identification and demonstrate the need for a live-cell target-identification approach (Fig.1).

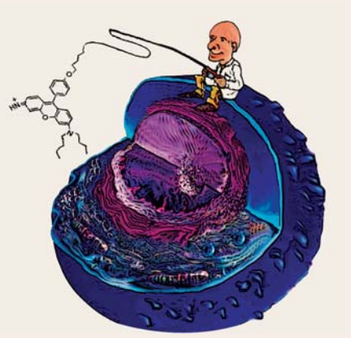

FIGURE 1. Target identification in a living cell. A living cell is composed of highly ordered structures in which small-molecule localization is precisely controlled by its chemical properties. Because of these intracellular barriers, binding proteins identified in in vitro experiments may not show the same effective binding in living cells.

Chemical biology has provided powerful tools to investigate complex biological systems.[1] It employs three disciplines:; small-molecule libraries, phenotype-based screening, and identification of protein binding-partners of small-molecule probes. Recent technological advances have greatly increased the number of small molecules and significantly enhanced screening capacity; however, identifying the binding-partners of small-molecule probes remains challenging.[2] A major difficulty lies in conventional target-isolation methods which require serious perturbation of the native cell environment, crucial for small-molecule localization and activity. Accordingly, only some proteins isolated from in vitro assays have shown effective binding to the same molecule in living cells. Here, we show this limitation of the in vitro target identification approach and demonstrate the importance of environmental factors in identifying fluorophore-binding proteins.

Previously we reported a fluorescent small-molecule capable of detecting differentiated myotubes from a mitochondria-targeted rosamine library.[3, 4] The hallmark of muscle differentiation is the fusion of mono-nucleated myoblasts to multi-nucleated myotubes.[5] During murine C2C12 myogenesis, the fluorescence intensity of one rosamine compound (I25 and I31; Fig. 2), increased significantly. This myotube selectivity may be achieved by binding to one of the differentiation markers expressed more highly in myotubes; alternatively, the probe may detect other physiological changes after differentiation.

In order to identify protein binders of these compounds, affinity matrices were prepared based on structure-activity relationship studies (Fig. 3a). Affinity pull-down assay is the most conventional method for identification of small-molecule binding protein.[6] It provides a straightforward methodology to isolate protein-binders from homogenous protein mixtures depending on binding affinity.[7] Affinity resins were incubated with myotube lysates and washed with buffer to get rid of non-specific binders. Then resin-bound proteins were separated by SDS-PAGE and stained with Coomassie blue (Fig. 3b). One enriched protein band at approximately 54 kDa was observed along with several other bands. To determine the specificity of protein-binders to these compounds, competition assay was followed. Myotube cell lysate was pre-incubated with 100 μM of I25, I31, rhodamine 123, or rhodamine B before affinity pull-down.

The strongest band at 54 kDa completely disappeared upon competition with unmodified I25 or I31, but not with rhodamine 123 or rhodamine B, which were included as structurally similar controls. Thus, we concluded that the 54 kDa band was the most convincing binding target protein of the compounds. The band was excised, sequenced, and identified to be tubulin. While affinity pull-down assays identified the major binder to be tubulin, a well-known cytosolic protein, our compounds appeared to be localized to mitochondria in live cells. The presence of tubulin in the mitochondrial membrane has been reported by a few groups,[8] but its suggested amount is only 2% of total tubulin in cells. Therefore, it was necessary to re-examine the endogenus binding target in the context of live cells.

For live-cell investigation, we synthesized a cell-permeable chemical affinity derivative, which has a thiol reactive chloroacetyl group, to enable covalent binding to target proteins (Fig. 3c). The compound is named CDy2 (Compound of Designation yellow 2) following the biological convention of Cluster of Designation (CD) for cell-surface markers. The benefit of the chemical affinity probe is that once it forms a covalent bond with its targets in live cells, those labeled proteins can be visualized by scanning the SDS-PAGE gel with a fluorescence scanner, even though the proteins are denatured.

When applied to myoblasts and myotubes, CDy2 showed a 2.3-fold increase in fluorescence intensity after differentiation (2.3±0.4 fold increase, N = 3; Fig. 3d), which is comparable to the increases observed with I25 and I31. To unveil the endogenus binding protein(s), myoblasts or myotubes were incubated with CDy2 for 1 hour. Labeled lysates were separated by SDS-PAGE and analyzed with a fluorescence scanner (Fig. 3d). Again, a unique fluorescently-labeled band was observed around 54 kDa (Fig. 3e). Also, pre-treatment of myotubes with I31 reduced the intensity of CDy2-labeled protein band, indicating effective competition of CDy2 with I31 in live cells. To determine

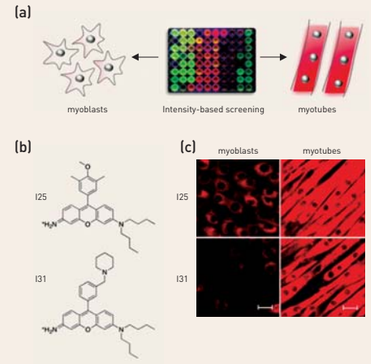

FIGURE 2. Probes for myogenic differentiation. (a) Screen of rosamine library. Myoblasts or myotubes were incubated with 500 nM of library compounds for 2 hours before imaging (b) Chemical structures of selected probes, I25 and I31. (c) Fluorescent images of I25 and I31 before (right) and after (left) muscle differentiation. Scale bar = 20 μm.

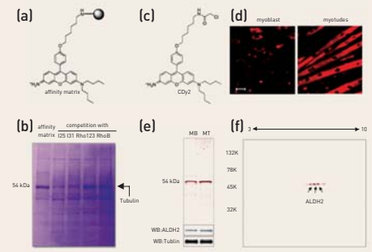

FIGURE 3. Identification of protein-binders in vitro vs in living cells. (a) Chemical structure of the affinity matrix used to isolate cellular proteins. (b) SDS-PAGE analysis of bead-bound proteins from C2C12 myotubes. In a competition assay, myotube lysates were pre-incubated with 100 μM of I25, I31, or control compounds (rhodamine 123 and rhodamine B) before the affinity pull-down experiment. (c) Chemical structure of CDy2 for labeling target protein in living cells. (d) Myoblasts (MB) or myotubes (MT) were incubated with CDy2 (500 nM) for 30 min and imaged with a fluorescent microscope. Then cells were lysed for in-gel fluorescence analysis (λ_{ex} = 530 nm, λ_{ex} = 580 nm). (e). (f) 2D-gel analysis for the identification of labeled-protein.

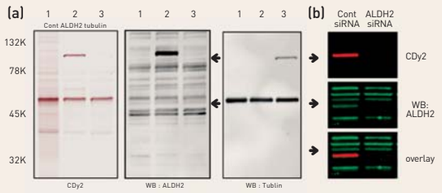

FIGURE 4. Validation of labeled protein identity in living cells. (a) GFP-tagged ALDH2 or tubulin constructs were transfected into HEK293 cells. After 48 hours, cells were labeled with CDy2 and subjected to in-gel fluorescence imaging. Immunoblot analysis shows the endogenous (black arrow) and over-expressed (red arrow) proteins; the HEK293 cell line was chosen because of its relatively high transfection efficiency.. (b) C2C12 myoblasts were transfected with siRNA against ALDH2. After 72 hours of transfection, cells were labeled with CDy2. Fluorescence labeling patterns of CDy2 were directly compared to ALDH2 immunofluororescence (green).

the identity of the labeled protein, cell lysates were separated by 2D-gel electrophoresis, and fluorescently-labeled spots around 54 kDa were excised and sequenced. To our surprise, the major spots were identified to be mitochondrial aldehyde dehydrogenase (ALDH2), eventhough tubulin is far more abundant in cells (10 ~ 20 μM).[9]

To validate the binding in living cells, firstly ALDH2 expression was suppressed by siRNA (Fig. 4b). Upon ALDH2 knock-down, the CDy2-labeled band (54 kDa) effectively disappeared. This implies that its binding to ALDH2 is exclusive; it does not label tubulin even in the absence of ALDH2. Secondly, ALDH2 or tubulin was overexpressed in HEK cells. Each protein was tagged with green fluorescent protein (GFP) to distinguish them from the endogenous proteins. Forty-eight hours after transfection, cells were labeled with CDy2 and each lysate was subjected to SDS-PAGE analysis (Fig. 4a). Again the result obviously shows that in living cells CDy2 labeled ALDH2-GFP, but not tubulin-GFP. Interestingly, when treated to cell lysates, CDy2 labeled tubulin instead of ALDH2. This result strongly suggests that CDy2 binds to two distinct proteins depending on the assay conditions; if treated to cell lysates, CDy2 labels tubulin as shown in affinity matrices, but if treated to live cells, it labels ALDH2. Taken together, these results suggest that ALDH2 is a binding protein of our muscle differentiation probes in the native environment.

Interestingly, the total amount of ALDH2 before and after differentiation remained unchanged (Fig. 3e), while in-gel fluorescence analysis showed that ALDH2 in myotubes is more strongly stained by CDy2. Thus it was necessary to determine the mechanism of selectivity of CDy2 for myotubes over myoblasts. For example, the mitochondrial membrane potential of skeletal muscle is quite high, possibly due to increased energy requirements for muscle contractions;[5] this elevated membrane potential may cause the myotube-selectivity of CDy2. In fact, when cells were fixed with formaldehyde, CDy2 lost its mitochondrial preference, as well as its selectivity for myotubes (Fig.5a). Further, the mitochondrial membrane potential was disrupted by treating cells with the mitochondrial uncoupler CCCP (carbonyl cyanide 3-chlorophenylhydrazone).[10] Upon pre-treatment with CCCP, the amount of fluorescently-labeled protein was significantly reduced (Fig.5b). These results support the notion that an increase in the mitochondrial membrane potential as a result of myogenesis gives rise to the selectivity of CDy2 for myotubes.

Rosamine compounds are derivatives of rhodamine and have long been used as mitochondrial probes. Their aromatic and cationic properties direct them to mitochondria due to the membrane potential across its bilayer.[4, 11] The rosamine probes are sensitive to the incresed membrane potential after myogenic differentiation. Once localized in mitochondria, they labeled ALDH2 selectively; the saturation curve of CDy2 against ALDH2-labeling revealed a dissociation constant (KD) of 1.4 μM. Although ALDH2 itself is not a differentiation marker, the fluorophore selectivity to a

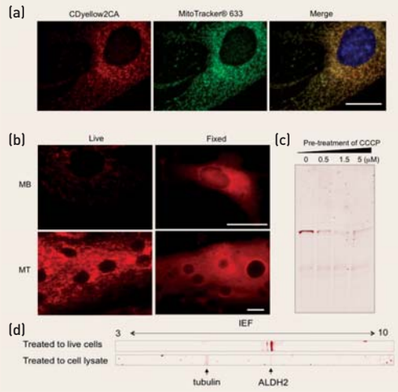

FIGURE 5. CDy2 localizes to the mitochondria. (a) A C2C12 myoblast labeled with CDy2 and co-stained with MitoTracker® Deep Red 633 (false-colored green here). (b) Live-cell versus fixed-cell images of CDy2. For live-cell images, myoblasts and myotubes were incubated with CDyellow2CA (500 nM) for 30 min. For fixed-cell images, cells were fixed with formaldehyde before labeled with CDy2. Scale bar = 20 μm. (c) To disrupt mitochondrial membrane potential, myotubes were pre-incubated with CCCP for 30min before CDy2 labeling. Cell lysates were subjected to in-gel fluorescence analysis. CDy2 labeling was effectively decreased with the pretreatment of CCCP. (d) Due to the difficulty of distinguishing ALDH2 and tubulin by size, isoelectric focusing (IEF) was conducted. When treated to living cells CDy2 strongly labeled ALDH2 (pI 7), but the band almost disappeared when treated to cell lysate. Instead, a new band appeared around pI 5, which was identified to be tubulin.

mitochondrial protein deserves careful consideration. Up until now, it has generally been believed that rhodamine dyes stain the mitochondrial membrane without showing specific interactions with mitochondrial proteins.[12]

A cell is a highly ordered structure[13] in which small-molecule localization is precisely controlled based on chemical properties. Accordingly, proteins that bind to a small molecule in vitro may not show effective binding to the molecule in living cells. In this study, CDy2 showed a prominent binding affinity to tubulin in vitro; however, the interaction was completely prohibited in living cells. This suggests that CDy2 is sequestered in mitochondria so rapidly that all CDy2 molecules are transported into mitochondria before the dye has a chance to react with tubulin in the cytoplasm. Though most commonly used, the in vitro pull-down approach can give misleading information about the probe-binding protein. Live-cell target labeling techniques have been introduced in recent studies;[14] however, their importance has not yet been fully addressed. Our observations strongly suggest that target identification in living cells can be crucial for identifying unknown protein-binder(s) of small-molecule fluorophores.

REFERENCES

1. Schreiber, S. L. Bioorg. Med. Chem. 1998, 6, 1127-1152.
2. (a) Asami, T.; Nakano, T.; Nakashita, H.; Sekimata, K.; Shimada, Y.; Yoshida, S. J. Plant Growth Regul. 2003, 22, 336-349; (b) Crews, C. M.; Splittgerber, U. Trends Biochem. Sci. 1999, 24, 317-320; c) Kim, Y. K.; Chang, Y. T. Mol. Biosyst. 2007, 3, 392-397.
3. Ahn, Y. H.; Lee, J. S.; Chang, Y. T. J. Am. Chem. Soc. 2007, 129, 4510-4511.
4. Kim, Y. K.; Ha, H. H.; Lee, J. S.; Bi, X.; Ahn, Y. H.; Hajar, S.; Lee, J. J.; Chang, Y. T. J. Am. Chem. Soc. 2010, 132, 576-579.
5. Chen, L. B. Annu. Rev. Cell Biol. 1988, 4, 155-181.
6. Haugland, R. P. The Handbook?A Guide to Fluorescent Probes and Labeling Technologies. Chapter 2.; 10th ed.; Invitrogen, 2005.
7. Walsh, D. P.; Chang, Y. T. Chem. Rev. 2006, 106, 2476-2530.
8. (a) Carre, M.; Andre, N.; Carles, G.; Borghi, H.; Brichese, L.; Briand, C.; Braguer, D. J. Biol. Chem. 2002, 277, 33664-33669; (b) Bernier-Valentin, F.; Aunis, D.; Rousset, B. J. Cell Biol. 1983, 97, 209-216; (c) Bernier-Valentin, F.; Rousset, B. J. Biol. Chem. 1982, 257, 7092-7099; d) Bhattacharyya, B.; Wolff, J. Nature 1976, 264, 576-577.
9. Hiller, G.; Weber, K. Cell 1978, 14, 795-804.
10. Chen, X.; Jennings, D. B.; Medeiros, D. M. J. Bioenerg. Biomembr. 2002, 34, 397-406.
11. (a) Johnson, L. V.; Walsh, M. L.; Bockus, B. J.; Chen, L. B. J. Cell Biol. 1981, 88, 526-535; b) Johnson, L. V.; Walsh, M. L.; Chen, L. B. Proc. Natl. Acad. Sci. USA 1980, 77, 990-994.
12. Jakobs, S. Biochim. Biophys. Acta. 2006, 1763, 561-575.
13. Holy, J.; Perkins, E. Structure and Function of the Nucleus and Cell Organelles; Humana Press, 2009.
14. (a) Rosania, G. R.; Chang, Y. T.; Perez, O.; Sutherlin, D.; Dong, H.; Lockhart, D. J.; Schultz, P. G. Nat. Biotechnol. 2000, 18, 304-308; (b) Tsukiji, S.; Miyagawa, M.; Takaoka, Y.; Tamura, T.; Hamachi, I. Nat. Chem. Biol. 2009, 5, 341-343; (c) Cravatt, B. F.; Wright, A. T.; Kozarich, J. W. Annu. Rev. Biochem. 2008, 77, 383-414.

PUBLICATIONS

1 Graphene-Based Multifunctional Iron Oxide Nanosheets with Tunable Properties

Chemistry a European Journal 2011, 17, 1214-1219

Hye Young Koo, Ha-Jin Lee, Hye-Ah Go, Young Boo Lee, Tae Sung Bae, Jun Kyung Kim, Won San Choi

We report the synthesis of graphenes with tunable properties due to the growth of needlelike iron oxide (IO) nanoparticles on their surfaces. The electrical conductivity, flexibility, and magnetic properties of graphene nanosheets (GNSs) could be tuned on demand by fine controlling both the surface coverage and the length of the IO nanoneedles. The degree of coverage of the IO nanoparticles on the surface of the GNSs made it possible to control the resulting properties of the IO/GNSs on demand. As examples of their utility, paperlike materials were generated by simple filtration, and the resulting IO/GNS nanocomposites showed extraordinary removal capacity and fast adsorption rates for AsV and CrVI ions in water. Another possible application is the preparation of multifunctional films equipped with conductivity, flexibility, and magnetic properties. The fabrication process is easy to scale up at a low cost. In addition, both the colloidal solution and film forms of the resulting IO/GNSs were effective for removal of heavy metal ions, meaning this material could be utilized for actual industrial applications.

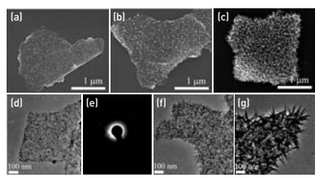

FIGURE 1. Electron microscopic images of IO/GNSs showing controlled morphology. a)-c) SEM images of the IO/GNSs upon repetition of re- ACHTUNGTRENUNGaction cycles 1, 3 and 5 times, respectively. d) TEM images of the IO/ GNS with one repetition of the reaction cycles. e) Selected area electron diffraction (SAED) pattern obtained from image d) f) and g) TEM images of the IO/GNS with three and five repetitions of the reaction cycles, respectively. One reaction cycle for the growth of the IO nanoneedles on the surface of GNS is an incubation with a mixed precursor solution of Fe2+ and Fe3+ (5 mL of a FeSO4 solution (1.9_10_5m) +5 mL of a Fe2ACHTUNGTRENUNG(SO4)3 solution (2.1_10_5m)) for 4 h.

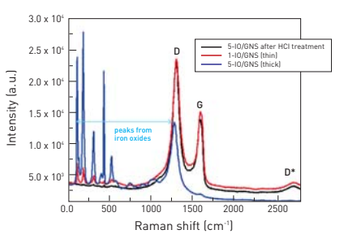

FIGURE 2. Raman spectra of the 1-IO/GNSs (red), 5-IO/GNSs (blue), and 5-IO/GNSs after removal of the IO by HCl treatment (black). The graphitic peaks of GNSs disappeared when there was a thick covering of IOs (5-IO/GNSs) and reappeared when the IOs on the surfaces were removed.

2 High-Performance Micro-Solid Oxide Fuel Cells Fabricated on Nanoporous Anodic Aluminum Oxide Templates

Advanced Functional Meterials 2011, 21, 1154-1159

Chang-Woo Kwon , Ji-Won Son , Jong-Ho Lee , Hyun-Mi Kim , Hae-Weon Lee , and Ki-Bum Kim

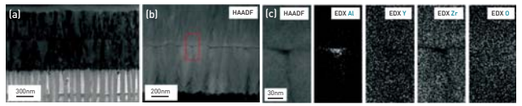

FIGURE 1. (a) Transmission electron microscopy (TEM) cross sectional images of ALD-modified 600 nm-thick YSZ films deposited by PLD on a porous AAO substrate with 40 nm pores: bright field image, (b) high angle annular dark field (HAADF) image, and (c) energy dispersive X-ray spectroscopy (EDX) elemental mapping images.

FIGURE 2. (a) OCVs of AAO-supported cell with a 300-, 600-, and 900-nm-thick total electrolyte layer with and without ALD modification, and (b) current-voltage curves of AAO-supported cell with ALD-modifi ed 900-nm-thick electrolyte layer at 400, 450, and 500 °ΔC.

Micro-solid oxide fuel cells (micro-SOFCs) are fabricated on nanoporous anodic aluminum oxide (AAO) templates with a cell structure composed of a 600-nm-thick AAO free-standing membrane embedded on a Si substrate, sputter-deposited Pt electrodes (cathode and anode) and an yttria-stabilized zirconia (YSZ) electrolyte deposited by pulsed laser deposition (PLD). Initially, the open circuit voltages (OCVs) of the AAO-supported micro-SOFCs are in the range of 0.05 V to 0.78 V, which is much lower than the ideal value, depending on the average pore size of the AAO template and the thickness of the YSZ electrolyte. Transmission electron microscopy (TEM) analysis reveals the formation of pinholes in the electrolyte layer that originate from the porous nature of the underlying AAO membrane. In order to clog these pinholes, a 20-nm thick Al2O3 layer is deposited by atomic layer deposition (ALD) on top of the 300-nm thick YSZ layer and another 600-nm thick YSZ layer is deposited after removing the top intermittent Al2O3 layer. Fuel cell devices fabricated in this way manifest OCVs of 1.02 V, and a maximum power density of 350 mW cm-2 at 500 oC.

3 Tumor-homing photosensitizer-conjugated glycol chitosan nanoparticles for synchronous photodynamic imaging and therapy based on cellular on/off system

Biomaterials 21 (2011) 4021-4029

So Jin Lee, Heebeom Koo, Dong-Eun Lee, Solki Min, Seulki Lee, Xiaoyuan Chen, Yongseok Choi, James F. Leary, Kinam Park, Seo Young Jeong, Ick Chan Kwon, Kwangmeyung Kim, Kuiwon Choi

Herein, we developed photosensitizer, protoporphyrin IX (PpIX), conjugated glycol chitosan (GC) nanoparticles (PpIXeGCeNPs) as tumor-homing drug carriers with cellular on/off systems for simultaneous photodynamic imaging and therapy. In order to prepare PpIXeGCeNPs, hydrophobic PpIXs were chemically conjugated to GC polymer whereupon the amphiphilic PpIXeGC conjugates formed a stable nanoparticle structure in aqueous conditions, wherein conjugated PpIX molecules formed hydrophobic innercores and were covered by hydrophilic GC polymer shells. Based on the nanoparticle structure, PpIXeGCeNPs showed a self-quenching effect that is an 'off' state with no fluorescence signal and phototoxicity with light exposure. This is due to the compact crystallized PpIX molecules in the nanoparticles, as confirmed by dynamic light scattering and X-ray diffraction methods. However, after cellular uptake, compact nanoparticle structure gradually decreased to generate a strong fluorescence signal and singlet oxygen generation when irradiated. Importantly, PpIXeGCeNP-treated tumor-bearing mice presented prolonged blood circulation, enhanced tumor targeting ability, and improved in vivo therapeutic efficiency, compared to that of free PpIX-treated mice. These results proved that this tumor-homing cellular 'on/off' nanoparticle system of PpIXeGCeNPs has great potential for synchronous photodynamic imaging and therapy in cancer treatment.

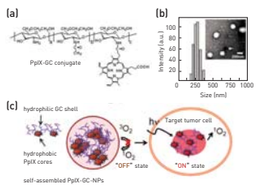

FIGURE 1. Design and characterization of PpIXeGCeNP. (a) The chemical structure of PpIXeGCeNP. (b) Size and shape of PpIXeGCeNP determined by DLS and TEM image. (c) Scheme diagram of self-assembled PpIXeGCeNP and cellular 'on/off' system for synchronous photodynamic imaging and therapy of cancer.

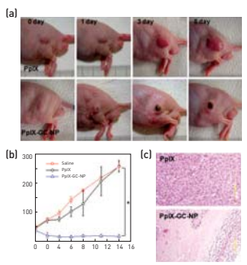

FIGURE 2. In vivo photodynamic therapy with PpIXeGCeNP. (A) Tumor images of free PpIX and PpIXeGCeNP (20 mg/kg of PpIX) in photodynamic therapy. (B) Measured tumor growth for 14 days (n ® 5). Data represent mean s.e. [* ®˜ p ← 0.01 by one-way ANOVA).

4 One-pot preparation of hydroxylated potassium organotrifluoroborates and subsequent Jones oxidation to potassium organocarbonyltrifluoroborates

Tetrahedron Vol.67 Issue 6, 2011, 1062-1070

Dong-Su Kim, Krishnavenu Bolla, Seokjoon Lee, Jungyeob Ham

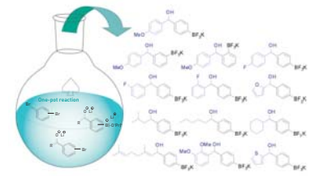

FIGURE 1. Sequential one-pot preparation of secondary alcohol-substituted potassium organotrifluoroborates from dibromobenzenes and various aldehydes.

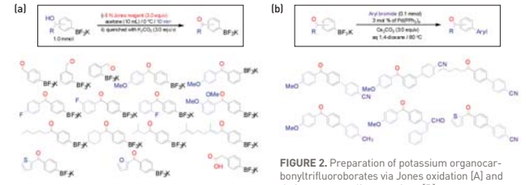

FIGURE 2. Preparation of potassium organocarbonyltrifluoroborates via Jones oxidation (A) and their cross-coupling reactions (B).

Potassium organotrifluoroborate salts have been recognized as useful synthetic reagents in the Suzuki-Miyaura cross-coupling reaction. Recently, methods for the direct functionalization of organotrifluoroborates, using their property of inertness under various reaction conditions, has been developed and used for the preparation of more complex organotrifluoroborates, which may be difficult to prepare by conventional syntheses of organoboron reagents. As part of the study to prepare functionalized potassium organotrifluoroborates, we discovered that potassium organocarbonyltrifluoroborates are readily obtained from the treatment of primary or secondary alcohol-containing organotrifluoroborates with Jones reagent.

In this paper, we report a facile one-pot synthesis of secondary alcohol-containing organotrifluoroborates from their corresponding dibromobenzenes, followed by the convenient preparation of potassium organocarbonyltrifluoroborates via Jones oxidation and the cross-coupling reactions of these organocarbonyltrifluoroborates in the presence of 3 mol % Pd(PPh3)4 catalyst at 100 oC.

5 Highly stable enzyme precipitate coatings and their electrochemical applications

Biosensors & Bioelectronics Vol.26, No.5, 2011, 1980-1986

Byoung Chan Kim, Xueyan Zhao, Hye-Kyung Ahn, Jae Hyun Kim, Hye-Jin Lee,Kyung Woo Kim, SujithNair, Erik Hsiao, HongfeiJia, Min-Kyu Oh, Byoung In Sang,Beom-Soo Kim, Seong H. Kim, Yongchai Kwon, Su Ha, Man Bock Gu,Ping Wang,Jungbae Kim

This paper describes highly stable enzyme precipitate coatings (EPCs) on electrospun polymer nanofibers and carbon nanotubes (CNTs), and their potential applications in the development of highly sensitive biosensors and high-powered biofuel cells. EPCs of glucose oxidase (GOx) were prepared by precipitating GOx molecules in the presence of ammonium sulfate, then cross-linking the precipitated GOx aggregates on covalently attached enzyme molecules on the surface of nanomaterials. EPCs-GOx not only improved enzyme loading, but also retained high enzyme stability. For example, EPC-GOx on CNTs showed a 50 times higher activity per unit weight of CNTs than the conventional approach of covalent attachment, and its initial activity was maintained with negligible loss for 200 days. EPC-GOx on CNTs was entrapped by Nafion to prepare enzyme electrodes for glucose sensors and biofuel cells. The EPC-GOx electrode showed a higher sensitivity and a lower detection limit than an electrode prepared with covalently attached GOx (CA-GOx). The CA-GOx electrode showed an 80% drop in sensitivity after thermal treatment at 50 °ΔC for 4 h, while the EPC-GOx electrode maintained its high sensitivity with negligible decrease under the same conditions. The use of EPC-GOx as the anode of a biofuel cell improved the power density, which was also stable even after thermal treatment of the enzyme anode at 50 °ΔC. The excellent stability of the EPC-GOx electrode together with its high current output creates new potential for the practical applications of enzyme-based glucose sensors and biofuel cells.

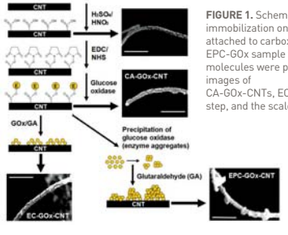

FIGURE 1. Schematic illustration of three different approaches to GOx immobilization on carbon nanotubes.GOx molecules were covalently attached to carboxylated CNTs via a linker ofEDC/NHS (CA-GOx). The EPC-GOx sample was prepared using the GA treatment after GOx molecules were precipitated in the vicinity of CA-GOx-CNTs. The SEM images of CA-GOx-CNTs, EC-GOx-CNTs, and EPC-GOx-CNTs are shown at each step, and the scale bar in each SEM image denotes 200 nm.

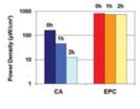

FIGURE 2. The power densities of biofuel cells with CA-GOx-CNT and EPC-GOx-CNTelectrodes, and their stabilities after thermal treatment at 50 °ΔC.

6 The Binding of Fluorophores to Proteins Depends on the Cellular Environment

Angewandte chemie International Edition 2011, 50, 2761-2763

Yun Kyung Kim, Jun-Seok Lee, Xuezhi Bi, Hyung-Ho Ha, Shin Hui Ng, Young-hoon Ahn, Jae-Jung Lee, Bridget K. Wagner, Paul A. Clemons, and Young-Tae Chang

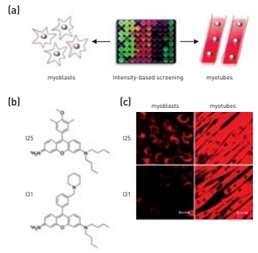

FIGURE 1. Probes for myogenic differentiation. a) Screen of rosamine library. Myoblasts or myotubes were incubated with 500 nm of library compounds for 2 h before imaging. b) Chemical structures of probes I25 and I31. c) Fluorescent images of I25 and I31 before (right) and after (left) muscle differentiation. Scale bar=20 mm.

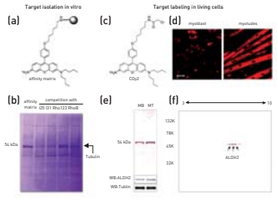

FIGURE 2. Identification of protein-binders in vitro vs. in living cells. (a) Chemical structure of the affinity matrix used to isolate cellular proteins. (b) SDS-PAGE analysis of bead-bound proteins from C2C12 myotubes. In a competition assay, myotube lysates were pre-incubated with 100 mM of I25, I31, or control compounds (rhodamine 123 and rhodamine B) before the affinity pull-down experiment. (c) Chemical structure of CDy2 for labeling target protein in living cells. (d) Myoblasts (MB) or myotubes (MT) were incubated with CDy2 (500 nM) for 30 min and imaged with a fluorescent microscope. Then, cells were lysed for in-gel fluorescence analysis (1ex = 530 nm, 1ex = 580 nm) (e). (f) 2D-gel analysis for the identification of labeled-protein.

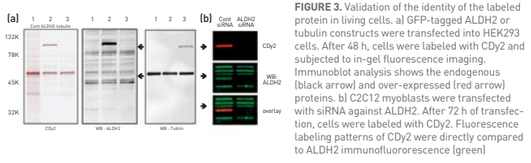

FIGURE 3. Validation of the identity of the labeled protein in living cells. a) GFP-tagged ALDH2 or tubulin constructs were transfected into HEK293 cells. After 48 h, cells were labeled with CDy2 and subjected to in-gel fluorescence imaging. Immunoblot analysis shows the endogenous (black arrow) and over-expressed (red arrow) proteins. b) C2C12 myoblasts were transfected with siRNA against ALDH2. After 72 h of transfection, cells were labeled with CDy2. Fluorescence labeling patterns of CDy2 were directly compared to ALDH2 immunofluororescence (green)

A living cell is a highly ordered structure, where small-molecule localization is precisely controlled based on chemical properties. Due to these intracellular barriers, targets identified in in vitro experiments may not show effective binding to the small molecule in living cells. In their communication in Agewandte Chemie, Y.K.Kim et al. describe a rosamine fluorophore that strongly binds to a cytosolic protein in vitro, however, if treated to live cells, it predominantly labels a mitochondrial protein.

PATENTS

TUMOR-TARGETING PROTEIN CONJUGATE AND A METHOD FOR PREPARING THE SAME

Patent No. **KR1043407** Key Inventor. **KWON, Ick Chan** (ikwon@kist.re.kr)

The present invention relates to a protein conjugate having excellent tumor-targeting capacity and a method for preparing the same. The present invention facilitates inclusion of a hydrophobic anti-cancer agent and can be combined with near-infrared fluorescent material.

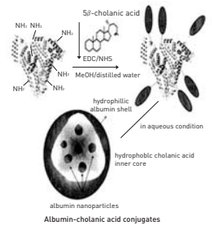

Albumin-cholanic acid conjugates

WIRELESS ELECTRICAL STIMULATING DEVICE FOR A LIVING BODY

Patent No. **KR1032269** Key Inventor. **Choe, Ilhwan** (kapil@kist.re.kr)

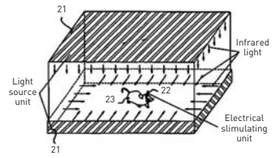

Mice are widely used for neurological studies due to an easier applicability of genetic manipulation. The small body size (7cm) and weight (25g) of the mouse renders relatively difficult the implementation of electrical stimulating devices with wireless capabilities in brain tissues. We designed a wireless-DBS system, mainly composed of a 1.3g-headset and illuminator.

ELECTROCONDUCTIVE PARTICLE AND ANISOTROPIC CONDUCTIVE FILM COMPRISING SAME

Patent No. **KR1018334** Key Inventor. **LEE, Sang-Soo** (s-slee@kist.re.kr)

The present invention discloses an electroconductive particle comprising (a) a polymer microparticle, and (b) a graphene coating layer grafted on a polymer microparticle, which has improved the long-term stability of conductivity, surface conductivity, durability, and thermal resistance, and is applicable for producing an anisotropic conductive film used for packaging electronic devices.

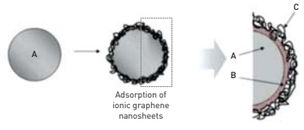

SOLAR CELL DEVICE COMPRISING A CONSOLIDATED CORE/SHELL POLYMER-QUANTUM DOT COMPOSITE AND METHOD OF THE PREPARATION THEREOF

Patent No. **KR1012089** Key Inventor. **Choi, Won-Kook** (wkchoi@kist.re.kr)

A high-efficiency solar cell device of the present invention comprising an active layer composed of a p-i-n form polymer-quantum dot composite having a consolidated core/shell structure. This device is capable of overcoming the shortcomings of conventional multi-layered solar cell devices.

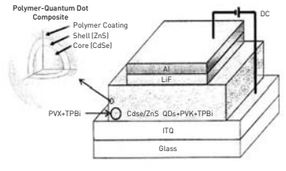

APPARATUS FOR DETECTING BRAIN CONDITIONS

Patent No. **KR1034798** Key Inventor. **Choi, Jee Hyun** (jeechoi@kist.re.kr)

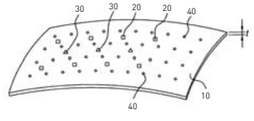

The apparatus for detecting brain conditions may include: a layer which is located adjacent to the brain of a living body; a light source which is formed on the layer and irradiates light to the brain; and an optical sensor which is formed on the layer adjacent to the light source and detects the light scattered from the brain. The apparatus for detecting brain conditions may be used to detect brain conditions such as cerebral oxygenation, cerebral blood volume, cerebral blood flow, etc. or to monitor brain activities, or to diagnose and/or localize the disease foci in case of neurovascular disease such as stroke including hemorrhage or bleeding, into or around the brain or brain tumors or epilepsy, etc.

ANTIGEN DETECTION KIT AND METHOD

Patent No. **KR1029343** Key Inventor. **AHN, Dae-Ro** (drahn@kist.re.kr)

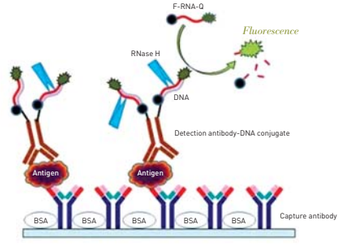

An antigen detection kit and an antigen detection method using the same are provided. The antigen detection kit comprises a capture antibody, a detection antibody bound to a single stranded DNA oligonucleotide, a single stranded RNA oligonucleotide complementary sequence to the DNA oligonucleotide, and an RNase

KIST NEWS

Indian Minister of Science and Technology Visits KIST

The Indian delegation of the Korea-India Joint Committee for Science and Technology, headed by Shri Pawan Kumar Bansal, the Minister of Science and Technology of India, and as well as speakers at the Korea-India Joint Workshop on Energy & Environment, visited KIST on May 2, 2011. This visit marked the 4th meeting of the Korea-India Joint Committee for Science and Technology.

The minister met with Dr. Kil-Choo Moon, President of KIST, and discussed joint cooperation and the current condition of the Korea-Indo Cooperation Center for Science and Technology. Since opening the Korea-Indo Cooperation Center for Science and Technology in Bangalore, India, in January 2010, KIST has been engaging in collaborative research projects and exchange of researchers and students. After the discussion, all visitors attended a Han River cruise hosted by Dr. Moon, who resolved to further strengthen cooperation between India and Korea.

Meeting for International Cooperation in S&T Development

A *'Meeting for International Cooperation in S&T Development'* was held on Wednesday, May 11, 2011, with foreign embassy science and technology representatives from developing countries. The main goals of the meeting were to initiate S&T development cooperation projects and strengthen network ties with participants.

Representatives from twenty countries, including the ambassadors of Colombia and Peru, attended the meeting, which included presentations by the Ministry of Education, Science & Technology (MEST) and KIST regarding the status and policy directions associated with their respective cooperation projects with developing countries.

Plans to set up a collaboration network of countries for S&T development, tentatively titled the Seoul S&T Club, were also discussed.

KIST Europe's Branch Lab Opens at KIST's Main Campus in Seoul

Dr. Andreas Manz, R&D Director at KIST Europe, established KIST Europe's Branch Lab at KIST's main campus in Seoul on June 9, 2011. The purpose of this lab is to promote collaborative research for micromachining technology using biological simulation technology.

This collaborative research will focus on the artificial simulation of blood cells or bacteria that are capable of exploring the regions of the human body and could be applied in the drug delivery or treatment of early lesions in the human body.

With the establishment of KIST Europe's Branch Lab in Seoul, the combination of EU's expertise in biotechnology and KIST's infrastructure is expected to create a synergistic effect for cooperative research.

Meanwhile, the Brain Science Institute at KIST, KIST Europe, and the Karlsruhe Institute of Technology have signed an agreement for mutual cooperation.

This MOU is a result of the Korea-EU High-level Networking Meeting, which was held in Germany in October of last year. The MOU is expected to promote cooperation and collaborative research in the fields of biotechnology and medicine using MEMS and nanotechnology.

KIST Participates in UKC 2011

KIST attended the US-Korea Conference 2011 (UKC 2011), held on August 10-14, 2011, at Park City, Utah, in celebration of the 40th anniversary of Korean-American Scientists and Engineers (KSEA).

KIST President Dr. Kil-Choo Moon delivered a presentation entitled "Working Together to Create the Future," discussing the advancement of science and technology and the future realization of creative "convergence."

In addition to participating in other various activities at the conference, KIST operated an information booth to promote KIST.

Chuseok Celebration 2011

Chuseok Celebration 2011 was held on September 7, 2011, to

celebrate Chuseok, one of the most important traditional holidays in Korea, as well as to provide opportunities for international scientists and students to experience Korean culture. About 250 international scientists, International R&D Academy students, professors and delegates of foreign embassies participated in the event. They enjoyed activities such as traditional Korean folk games, folk painting, traditional clothing contest, taekwondo demonstration, etc.

The dinner, hosted by Dr. Kil-Choo Moon, president of KIST, was joined by many diplomatic officers from foreign embassies including Ambassador Kamal Prasad Koirala of Nepal, Ambassador Desmond Akawor of Nigeria, Ambassador Dato Ramlan bin Ibrahim of Malaysia, and Ambassador CHAN Ky Sim of Cambodia.

Three teams of IRDA students came forward to showcase their talents in the talent show, and many prizes and gifts were handed out, including best dressed prizes to the winners of the traditional clothing contest. For the last event, a performance team from the Dong-A Media and Arts Institute performed a traditional "Kyunggi" folk song and gave a traditional "Nanta" drums and dance performance.

The seventh Vietnamese Students' Day in Korea at KIST

"The seventh Vietnamese Students' Day in Korea" was held successfully at KIST on 2 days 8th and 9th, Oct. 2011. This big event was organized by Vietnam embassy in Korea, Vietnamese Students' Association in Korea (VSAK) in co-operation with KIST and sponsored by Hanshin Engineering & Construction Co.Ltd. There were more than 700 participants attended in this event. Mr. Tran Hai Linh, the President of Vietnamese Students' Association in Korea, is delivering opening speech

Awards

- **Dr. Sang Bae LEE, Future Convergence Research Division**
  - Order of Science and Technology Merit / Doyak Medal (Ministry of Education, Science and Technology, April 21, 2011)
- **Dr. Myoung Woon Moon, Future Convergence Research Division**
  - The Won Hee Park Award (KIST, February 10, 2011)
- **Dr. Kyung Kon KIM, National Agenda Research Division**
  - KIST Staff of the Month (KIST, January 31, 2011)
- **Mr Dae Shin KANG, Research Planning & Coordination Division**
  - Minister Citation (Ministry of Education, Science and Technology, April 21, 2011)
- **Mr Yong Gwon KIM, Research Planning & Coordination Division**
  - Minister Citation (Ministry of Education, Science and Technology, April 21, 2011)
- **Mr Hwan LIM, Research Planning & Coordination Division**
  - Minister Citation (Ministry of Education, Science and Technology, April 21, 2011)
- **Dr. Jae Young CHOI, KIST Gangneung**
  - Minister Citation (Ministry of Environment, April 28, 2011)
- **Dr. Chang Joon LEE, Brain Science Institute**
  - KIST Staff of the Year 2011 (KIST, February 10, 2011)
- **Dr. Young-Jei OH, Future Convergence Research Division**
  - Award for Best Poster (MPA, June 29, 2011)
- **Dr. Hyeon Ok YANG, KIST Gangneung**
  - Award for Best Paper (Seoul National University, January 14, 2011)
- **Dr. Ju Young LEE, Functional Food Center**
  - Award for Best Paper (Seoul National University, January 14, 2011)
- **Dr. Hak Cheol KWON, Natural Medicine Center**
  - Award for Best Paper (Seoul National University, January 14, 2011)

A Sign of the Times!

Development Path of KIST

National Needs

- Fast industrialization by importing technologies and materials
- Developing major industrial technologies and advancing quality of life
- Ensuring the core competency for The 21st century knowledge-based economy
- Key industrial technologies, public & welfare technologies
- Frontier & fundamental technologies

KIST'S Role

- Adoption of advanced & modification of Imported technologies

US-Korea Contact on "Foundation of a research institute for Korea's growth in industrial technology and applied science" under US-AID Program (1965)

As Korea has transitioned from an aid receiving country into an aid-giving country, KIST is set to focus more on ODA projects.

KIST established

60~70

- Construction Plan for POSCO ('69)
- Development Plan for Automobile Industry ('70)
- Basic Plan for Shipbuilding Industry ('72)
- Color TV set ('72)
- Dongbok Steel Wire Manufacturing Technology ('76)
- Polyster Film ('78)

80~90

- Korea's first material patent, aramide pulp ('82)
- CFC Alternative Material ('83)
- Super Mouse ('88)
- Artificial Diamond ('88)
- Lyocell artificial silk Manufacturing Process ('92)
- Pheumonia Vaccine ('99)

2000~

- Hydro-Fuel Cell Car
- Capsule type Endoscope
- Natework-based Humannoid
- R&D in KIST
  HUb of Brain Science, Biomedical Research, Future convergence research,
  National agenda research

KIST ODA Activities

IRDA

- International R&D Academy(120 students) ('01~)

Project

- Vietnam, Project for the Establishment of Korea-Vietnam Technology Cooperation Center ('01)
- Indonesia, Establishment of Energy-Environment Research Center ('09~)
- Vietnam, Sharing Korean Development Experiences ('10~)
- China, Reduction of environmental stress by terrestrial pollutant control in the Yellow Sea ('08~)

Training

- Training program on Environmental Protection Technology and Management for Air Pollution Control ('94~)
- Vietnam, Training Course on R&D Management for VAST ('09)

Alumni Update

A little over six years ago (2005), while going through some of the top ranked research labs in neuroscience, I came across the Korea Institute of Science & Technology (KIST) and was thrilled to know that Dr. Shin Hee-Sup' s lab had very active research in the field of neuroscience. I picked his lab because everything was outstanding. I didn't know then that I had made a choice that would change my life.

I am confident to say that the Brain Science Institute at KIST was the right place for empowering me to fulfill my dreams. Studying at KIST, especially in the Brain Science Institute, was probably the best decision I ever made in my life. Getting an opportunity in an esteemed institute in the field of neuroscience allowed me a fair chance to explore new avenues of knowledge and fulfilled my desire of publishing a research article in a renowned journal like *Neuron*. All I now have was initially a big dream. I started on my career path with a series of smaller, achievable goals that eventually led me to major achievement.

Work on projects pushed my limits and stretched me beyond what I would have thought possible. If I had never come to KIST, I probably wouldn't have gotten the chance to meet Dr. Shin Hee-Sup, receive the grand prize from the University of Science & Technology (UST) as well as KIST' s Academic Excellence Award, or settle down into my current position as Star-Postdoctoral Researcher so quickly. I shall simply say that all is well that ends well.

I would like to thank many people on campus, from professors to the President; through their commitment to research, they have captured our interest, inspired and guided us to fulfill our dreams. In particular, I acknowledge my mentor, Dr. Shin Hee-Sup, Director-General of the Brain Science Institute, for his skillful guidance, intellectual vigor and amicable behavior throughout my research work. As my advisor, he gave his time and advice most generously, and made this achievement possible. His training has improved my ability to think precisely. His creative suggestions and expertise have inspired and motivated me to excel in the field of neuroscience.

Appreciation is extended to my friends and colleagues, who have provided unending encouragement, enthusiasm, and support throughout my stay at KIST. The unforgettable company of Dr. Adila Rani and Dr. Yasar Saleem, have never allowed me to feel alone or far from home and have provided a good source of friendship. Special thanks to my loving daughter, Momiza Tariq, whose lovely talk was a great source of encouragement and satisfaction during a long stay away from home. One of the most valuable lessons I learned at KIST is that by being ready to simply learn and just doing simple stuff can go a very long way. There are a few simple, but critically important lessons I' ve learned during my stay at KIST: First, we must believe in ourselves and in our work. Secondly, we must be confident and seek out the toughest jobs. Third, we must learn from our failures. Fourth, we must have a high threshold for frustration. Finally, we must follow whatever our passion is.

For more information for IRD A program at KIST. go to:
http:// irda.kist.re.kr

Regards,
Tariq Zaman

Editorial Information

Editors-in-Chief
Jun Kyung Kim

Editorial board members
Hae-Young Koh
Hyun Kwang Seok
Heedong Ko
Kyungkon Kim
Youngsoon Um
Seok Won Hong
Eun Gyeong Yang

Managing Editor
Han La Park
kistoday@kist.re.kr

Editorial office telephone
+82-2-958-6161

Web addresses
www.kist.re.kr
www.kist.re.kr/en

English Advisory Services
Anne Charlton

The Final Word Editing Services
the_final_word@live.com

KIST Korea Institute of Science and Technology

Korea Institute of Science and Technology
Cheong Ryang, P.O. Box 131, Seoul 136-650, South Korea